Title
The Effects of Hoja loca on Maize Organogenesis

Author
Sluis, Aaron Michael

Publication Date
2016

Peer reviewed|Thesis/dissertation

The Effects of *Hoja loca* on Maize Organogenesis

By

Aaron Michael Sluis

A dissertation submitted in partial satisfaction of the

requirements for the degree of

Doctor of Philosophy

In

Plant Biology

In the

Graduate Division

of the

University of California, Berkeley

Committee in charge:

Professor Sarah C Hake, chair
Professor Jennifer C Fletcher
Professor Michael R Freeling
Professor David A Weisblat

Spring 2016

Abstract

The Effects of *Hoja loca* on Maize Organogenesis

By

Aaron Michael Sluis

Doctor of Philosophy in Plant Biology

University of California, Berkeley

Professor Sarah C Hake, Chair

Plant organs initiate from meristems and grow into diverse forms. Initiation is followed by a morphological phase where organ shape is elaborated, and finally tissues differentiate into their mature state. This process involves a variety of mechanisms, including complex gene regulatory networks, intricate patterning of plant hormones, and dynamic tissue growth. *Hoja loca* is a maize mutant that has defects in initiating and forming leaves and other lateral organs. I aim to use the *Hoja loca* mutation to investigate processes involved in transitioning tissue from undifferentiated meristem to lateral organs. Its unique phenotype suggests that it can greatly aid the understanding of plant organogenesis due to the specificity of mutant defects to organ initiation.

In this dissertation, I investigate the effects of the *Hoja loca* mutation on shoot organogenesis in *Zea mays*. In Chapter 1, I describe the mutant phenotype. In Chapter 2, I identify the mutant locus. I use RNA-seq differential gene expression to look at global changes and identify genes that are likely to mediate the *Hoja loca* defect. In Chapter 3, I investigate the localization of genes and metabolites that are important in organogenesis, namely the patterning of auxin. Together, these results suggest that *Hoja loca* causes an auxin-insensitivity in part of the auxin signaling response, likely at the site of organ initiation. This change is signaling leads to the misexpression of a beta glucosidase capable of activating cytokinin glucoside conjugates, and potentially the degradation of flavonols. The balance of cytokinin and auxin is a critical regulator of tissue differentiation, and flavonols affect auxin transport. Disrupting the localization of either of these compounds in the shoot could plausibly lead to the mutant phenotypes of skipped leaf initiation and altered leaf morphology.

Acknowedgements

Research reported in this publication was supported in part by the National Institutes of Health S10 program under award number 1S10RR026866-01. The content is solely the responsibility of the authors and does not necessarily represent the official views of the National Institutes of Health.

This research was funded in part by a National Institutes of Health NRSA Trainee appointment.

Introduction

Plant development proceeds as an iterative process of organ initiation from meristems. Above ground tissues originate from the shoot apical meristem (SAM), which initiates lateral organs in regular phyllotactic patterns. In all cases, a lateral organ is formed along with an axillary meristem, and often one or the other is suppressed (McSteen and Leyser 2005). This basic developmental unit is known as a phytomer, and aerial plant development can be understood as successive formation of phytomer units (Galinat 1959). Continual organ initiation allows plant architecture to be flexible and respond to changing environmental conditions, resulting in plants of the same species often differing greatly in organ number or organ size.

Organogenesis involves a subset of meristematic cells transitioning to determinate growth, requiring broad changes in cell physiology, transcriptional regulatory networks, and hormones. Cells that transition to organ initiation are within the peripheral zone – also called the morphogenetic zone – while cells that replenish the meristematic cells are in the central zone. The site of incipient organ formation is called the Plastochron 0, or P_0, used to index leaves at a point in development. As organs develop, various asymmetries are established that determine tissue identity across proximal/distal, abaxial/adaxial, and medial/lateral axes. The establishment of a boundary between the initiating organ and the rest of the meristem is essential to organogenesis and meristem maintenance.

The first step in organogenesis is establishing the position of organ initiation. The Hofmeister principle states that new organs form in the location maximally distant from previous primordia (Snow and Snow 1932). The plant hormone auxin is thought to be a central regulator of organ patterning given its concentration gradient patterns across the SAM (Benková et al. 2003). This patterning is achieved through polar auxin transport by PIN efflux proteins, which are named after their mutant phenotype of pin-like inflorescences devoid of lateral organs (Okada et al. 1991). Although the inflorescence phenotype is the most conspicuous, subtle phyllotactic defects exist in the vegetative shoot of *pin* mutants (Guenot et al. 2012). Feedback between auxin and PIN patterning leads to the formation of local auxin concentration maxima as PIN polarization in the epidermis directs auxin flow toward regions of higher auxin concentration (Heisler et al. 2005). At the position of auxin maxima in the P_0, a switch occurs in which auxin moves internally, thus creating an incipient vascular strand that will connect with older strands and form an auxin sink. These feedback systems lead to the dynamic pattern formation necessary to create auxin maxima, which ultimately lead to observed phyllotactic patterns.

Auxin moves throughout plants by a variety of mechanisms. Auxin will freely enter cells from a protonated state in acidic cell walls, but become charged in the neutral cytoplasm. Thus, auxin will move into cells via a chemiosmotic mechanism (Rubery and Sheldrake 1974). Auxin transporters, including ABCB

proteins, AUX1/LAX family members, and PIN proteins are required for auxin efflux, and also assist in influx (Noh, Murphy, and Spalding 2001; Friml et al. 2003; Petrášek et al. 2006; B h Lee et al. 2009; Zažímalová et al. 2010; Peer et al. 2011). As efflux is the limiting step in auxin movement, the PIN proteins mediate auxin movement in many developmental contexts (Adamowski and Friml 2015). While there are a variety of conserved PIN proteins in plants, PIN1 has the greatest effects on shoot patterning (Okada et al. 1991).

Models have attempted to reconcile how one protein, PIN1, can move auxin flow up concentration gradients toward the P_0 as well as flow along paths of auxin flux away from maxima in vasculature (Wabnik et al. 2011; Bayer et al. 2009). The *MAB4* gene family, which encode NONPHOTOTROPIC HYPOCOTYL 3-like proteins and regulate PIN endocytosis, provides a possible explanation for this switch in *Arabidopsis*. MAB4 was found to play a critical role in PIN patterning by directing polarization internally at the site of organ initiation in the direction of auxin flux (Furutani, Nakano, and Tasaka 2014). MAB4, along with related proteins MEL1 and MEL2, are involved in the regulation of PIN polarity (Furutani et al. 2011). *mab4 mel1 mel2* triple mutants have a pin-like inflorescence and altered PIN1 localization. PIN1 patterning is normal in the epidermis of the triple mutant meristem and leads to an auxin convergence, but internal expression from the auxin maximum to sink tissue is absent. Without a sink, auxin accumulates at the meristem surface. MAB4 expression depends on auxin signaling and is upregulated at the site of organ initiation in wild-type plants. Together, these observations demonstrate a mechanism that reconciles different modes of PIN1 polarization and auxin distribution: high auxin levels turn on MAB4 and trigger a switch from up-the-gradient to with-the-flux PIN polarization at the site of initiation (Furutani, Nakano, and Tasaka 2014).

Auxin signaling begins with auxin perception. In the nucleus, auxin facilitates the binding of Aux/IAA genes to the $SCF^{TIR1/AFB}$ complex (Gray et al. 2001). This interaction was demonstrated with *axr2*-GUS and *axr3*-GUS (IAA7 and IAA17, respectively) reporter constructs carrying mutations in domain II that result in much higher expression than constructs with wild-type sequence. These constructs also conferred auxin-related growth phenotypes like leaf curling and reduced apical dominance. Similar effects could be observed from non-mutant AXR2-GUS overexpressed constructs in the *tir1* mutant background. The interaction of Aux/IAA proteins with TIR1 was confirmed with immunoprecipitation, and domain II was shown to be necessary and sufficient for binding (Gray et al. 2001). Auxin directly enhances the interaction between $SCF^{TIR1/AFB}$ and the domain II, demonstrating that this complex is an auxin receptor (Dharmasiri, Dharmasiri, and Estelle 2005; Kepinski and Leyser 2005). Variation in the auxin-facilitated binding affinity of Aux/IAA alters the auxin concentration necessary to promote transcriptional responses, thus fine-tuning auxin responses (Calderón Villalobos et al. 2012).

Given the above data, it appears clear that domain II of Aux/IAA proteins controls protein stability. A 13-amino acid sequence is sufficient to target proteins for degradation in a proteasome-inhibitor dependent manner (Ramos et al. 2001). A variety of mutations in this region cause striking developmental effects (Reed 2001).

Aux/IAA protein domains III and IV share sequence similarity with many auxin response factors (ARFs), and indeed these proteins can bind each other (Ulmasov, Hagen, and Guilfoyle 1997). ARFs bind DNA at auxin responsive elements (*AuxREs*) and function as transcriptional activators and repressors (Ulmasov et al. 1995; Boer et al. 2014). When an Aux/IAA protein is bound to an ARF, the TPL corepressor and chromatin modifiers are recruited to downregulate gene expression (Tiwari, Hagen, and Guilfoyle 2004; Szemenyei, Hannon, and Long 2008). Domain I of Aux/IAA proteins contain an EAR motif and mediates this transcriptional repression. Degradation of Aux/IAA protein by auxin signaling frees ARFs to bind target DNA and effect transcriptional responses. AUX/IAA and ARF interactions are likely more complicated than simple dimerization; Aux/IAA multimers are required for proper signaling repression (Korasick et al. 2014; Nanao et al. 2014).

Many factors affect auxin signaling, making the process difficult to study. The simple combinatorial diversity of the main signaling proteins – 6 TIR1/AFB proteins, 29 Aux/IAA proteins, and 23 ARF proteins in *Arabidopsis* – is substantial (Peer 2013). Other gene regulatory networks feed into this pathway, as with the brassinosteroid signaling BIN2 kinase that phosphorylates ARF7, affecting binding with Aux/IAA partners (Cho et al. 2014). There is also significant feedback in auxin signaling, notably with PIN expression downstream of Aux/IAA and ARF regulation (Vieten et al. 2005). Cytokinin and auxin mutually regulate one another; exogenous auxin application or overexpression reduces cytokinin concentration and cytokinin oxidase expression (Eklöf et al. 2000), whereas cytokinin can positively or negatively affect auxin, in part via ethylene (Růzicka et al. 2007; Eliasson, Bertell, and Bolander 1989). This balance is seen during shoot organogenesis, where proper phyllotactic patterning requires inhibitory cytokinin fields (Besnard et al. 2014).

Of particular relevance to this thesis is the role of flavonoids in auxin patterning. Flavonoids are phenylpropanoic secondary metabolites. Flavonoid deficient mutants such as *transparent testa4* in *Arabidopsis* have increased polar auxin transport (PAT) and defects in root gravitropism (Buer and Muday 2004), whereas *transparent testa3* over-produces flavonoids and has decreased PAT (Peer et al. 2004). Further evidence for a role for flavonoids in auxin transport comes from work with the WRKY23 transcription factor. This factor lies downstream of ARF7 and ARF19 and directly stimulates local biosynthesis of flavonols (Grunewald et al. 2012). WRKY23 is necessary for organization of the primary root tip and for initiation of lateral roots. It is also required for the local production of flavonols at the site of lateral root initiation. These data suggest a

feedback where high auxin signaling induces flavonol production and limits auxin transport. This signaling does not affect PIN expression, but work with the *pin2* mutant again demonstrates an important role for flavonols, this time with the root gravitropic response (Santelia et al. 2008). Agravitropic *pin2* roots can be rescued by nanomolar application of flavonols.

A wide variety of flavonols exist in plants. There are two base flavonol aglycones: kaempferol and quercetin. These can receive a variety of sugar conjugations at the 3 and 7 carbon positions via UDP-dependent glycosyltranferases (UGTs) (Saito et al. 2013), resulting in an array of flavonol glycosides and bisglycosides. Careful analysis of Arabidopsis UGT mutants showed that kaempferol 3-O-rhamnoside-7-O-rhamnoside acts as an endogenous PAT inhibitor in shoots (Yin et al. 2014).

Flavonols likely affect auxin patterning post-transcriptionally. Quercetin acts as an endogenous inhibitor of the PINOID kinase, which mediates the polarized localization of PINs to the plasma membrane, thus modulating PAT (Henrichs et al. 2012). ABCB1/19 proteins bind quercetin *in vitro*, inhibiting ABCB1 auxin transport (Geisler and Murphy 2006). This action is likely similar to that of the synthetic auxin transport inhibitor NPA, which competes with quercetin for *in vitro* binding (Jacobs and Rubery 1988; Murphy et al. 2002).

Chapter 1 – Characterizing *Hoja loca*

Introduction

Zea mays is a monocot grass with a long history of study as a model organism due to its wide morphological diversity, plentiful seed set, and expansive collection of interesting mutants. The maize shoot has a relatively simple plant architecture consisting of alternating leaves coming from a stalk with minimal or no branching (Figure 1A). Branches that are made are called tillers, usually originating from the first few leaf nodes. The reproductive tissues consist of an apical male tassel and female ears originating from axillary buds.

Maize is particularly suited to investigations of plant development. The large SAM is easy to observe and has well defined flanks from which organs initiate in alternate distichous phyllotaxy. This makes maize especially suited to *in situ* hybridization, immunolocalization, and other histological methods.

Maize leaf morphology also provides excellent visualization of developmental growth axes. The proximal leaf sheath clasps the stem, while the distal blade lies flat to act as the primary photosynthetic surface. Separating these tissues is the ligule/auricle boundary. The auricle is an expanded region of tissue that acts as a hinge to permit the blade to extend away from the stem. The ligule is a fringe of tissue that clasps the stem to form a seal preventing water and debris falling between the sheath and stem. Disruptions to abaxial and adaxial patterning are also easy to observe, with specialized cell types such as macrohairs and bulliform cells indicating adaxial tissue. Finally, there is mediolateral patterning with a medial blade midrib and lateral leaf domains.

The maize inflorescences provide another opportunity to investigate the initiation of lateral organs, but with different phyllotaxy and organ type. At the floral transition, the SAM becomes an inflorescence meristem (IM) to begin forming the tassel. Instead of producing leaves, the IM produces branch meristems (BMs) and spikelet pair meristems (SPMs). BMs also produce SPMs. SPMs will initiate two spikelets, each with a floral meristem that produces the male flower. The ears are formed from axillary buds and usually do not form any branches.

The availability of diverse genetic backgrounds in maize adds utility to mutant investigation in this model species. Hundreds of stable inbred lines are available, providing variability in a wide set of traits. Many developmental mutants display different phenotypes depending on the inbred background. For instance, this variability was seen in Teopod mutants, leading to the suggestion that certain members were functionally distinct (Poethig 1988). Large changes in phenotypic variability are also observed, as with the *knotted1-E1* (*kn1-E1*) mutation, which makes limited, non-viable shoots in the W22 and W23 backgrounds, but is permissive in B73 and Mo17 (Vollbrecht, Reiser, and Hake 2000). This change

is attributed to the difference in meristem size between the inbreds which is mediated by multiple QTL (Thompson et al. 2015).

Results

Isolation of Hoja loca

Hoja loca was discovered by a traditional forward genetic approach. Ethyl methanesulfonate (EMS) was used to treat pollen of the Mo17 maize inbred that was crossed onto the B73 inbred. Hybrid F1 seed were planted in the field. EMS induces random mutations throughout the genome, specifically changing G:C nucleotide pairs into A:T pairs (Griffiths et al. 2000). Using hybrids in an EMS screen gives the mutants a hybrid advantage, thus weak mutants can survive (Neuffer et al. 2009). *Hoja loca* was selected for its distinctive phenotype (Figure 1B). The above-ground tissues of these mutants display a variety of growth defects that lead to gnarled and stunted plants. This appearance lead to the name *Hoja loca*, which means 'crazy leaf' in Spanish. Several of the mutant defects – including meristem abortion, tubular leaves, and reduced leaf count – suggested an interesting effect on meristem activity and organ initiation. The mutation is dominant and, with rare exception, female sterile.

A putative second allele was identified in another EMS screen, this time in the A619 inbred. This mutant has a very similar phenotype, but is less severe overall. Homozygotes of *Hoja loca 2* have more severe phenotypes than heterozygotes, showing that this mutation is antimorphic, or a dominant negative. The few recovered homozygotes of *Hoja loca 1* that have been observed have all had severe mutant phenotypes.

Variable penetrance of *Hoja loca*

The *Hoja loca* phenotype is highly variable and primarily affects the leaves. Scoring just the heterozygotes, mutants can broadly be classified into mild and severe groups. Mutants range from having no discernable phenotype – cryptic mutants – to aborting after only initiating the coleoptile. Mild plants have leaf numbers near that of wild type siblings, but display defects in leaf morphology, namely tubular leaves with fused margins and leaf blades that lack a midrib (Figures 4 and 5). In severe plants, the leaf number defect is much more pronounced, with some plants only producing a few leaves (Figure 1C and D). Severe mutants also have a greater portion of leaves with morphological defects. Formation and fertility of female ears is greatly reduced in all mutants.

Hoja loca was introgressed into different maize inbreds, with resulting variation in mutant penetrance. Most of the analysis in this thesis is done on mutants in the B73 background, the same inbred used to sequence the reference maize genome. This background displays a moderate severity, which facilitates mutant scoring and analysis of phenotypes. It is notable for mutants that have few or no tassel branches (Figure 1E). A619 displays similar penetrance, with a slight reduction in severe phenotypes. Mutants in W22 are highly tillered with a bushy

architecture (Figure 1F). W22 mutants also make highly feminized tassels. This is likely a result of their formation on tillers, which are often feminized in many maize backgrounds. *Hoja loca* in W22 is propagated by crossing wild-type pollen onto the feminized tassels, unlike the other inbred backgrounds which are propagated by pollen. A632 is notable for forming tube leaves around the 5th or 6th leaf (Figure 1G). This occurs in all backgrounds, but at a much higher rate in A632.

Variation also exists between particular families in the same inbred. A given cross will result in more or less average severity among siblings. Selecting individuals for crossing, whether for mild or severe plants, has little effect on the severity of progeny (Figure 2A). This suggests that many factors in the genetic background contribute to mutant severity, and differences among inbreds mediate this.

A generational effect is also observable when selfing or introgressing. F1 progeny display much milder mutant phenotypes, with many F1 showing no discernable phenotype. Subsequent generations display greater severity. In the case of the A619 introgression, mutants beyond the 4th backcross generation had reduced fertility to the point where introgression beyond the 5th generation was impractical. This effect made the generation of double mutants with *Hoja loca* impossible without reliable genotyping. Even when blindly selfing F1s, recovery of the *Hoja loca* mutant phenotype in the F2 generation was unsuccessful.

Mutant fertility is a particular challenge in analyzing *Hoja loca*. The mutation is dominant, so crosses must be made with mutants. Severe mutants that make few leaves will produce minimal inflorescences and are non-viable (Figure 1D). Mild mutants usually make both ears and tassels, but with rare exception only the tassels are fertile. Ears will often make silks, but usually will not bear seed (Figure 6E). Some mutant tassels will shed pollen, but many are sterile. In the B73 background, a typical planting of 20 mutant individuals, from 3 to 7 plants will shed, with perhaps one or two individuals doing so for more than one day. Difficulty in increasing seed is a persistent problem in *Hoja loca*, and necessitated a change from working with plants introgressed in the A619 background to introgression into B73 for analysis.

The following discussion of phenotypes uses mutants that have been well introgressed into B73.

Skipped Node Phenotype

A primary mutant defect is the failure to initiate a leaf at a shoot node. Wild type plants initiate a leaf at each node, totaling about 14 adult leaves for a mature plant. Mild mutants will have a slightly reduced leaf number, typically from 12 to 13 leaves (Figure 2B). Dissection of the plant reveals bare nodes where leaf initiation has failed (Figure 3A). Internode segments are found above and below this node, and no other changes to plant architecture are found. Severe plants

have many more skipped initiation events, often several in a row (Figure 3B). The first leaf is always initiated, except in the case of an aborted plant that only grows a coleoptile. The second leaf also appears to initiate at a greater rate, but less than the first. Subsequent nodes are roughly equally likely to initiate a leaf, as the process becomes stochastic (Figure 2C). A slight increase in leaf initiation rate is seen around the 7th node position, corresponding with resumption of leaf initiation upon germination.

Careful inspection shows that overall plant phytomer organization is undisturbed even in severe mutants. Upon the floral transition, internodes elongate and node positions become clearly visible (Figures 3B and 3G). The total number of nodes is consistent between wild type and mutant plants (Figure 2B). Splitting the stem laterally shows well-defined tissue differentiation at nodes (Figure 3C). In the case of mild mutants, phyllotaxy maintains an alternate pattern as though the leaf were properly initiated, thus adjacent leaves surrounding a skipped node will initiate from the same side (Figure 3D). Sometimes alternate phyllotaxy appears to be disrupted, but this is more likely attributable to the tendency for malformed leaves to trap the growing shoot within, thereby twisting and constraining the shoot (Figure 3E).

While internodes consistently form before and after skipped leaf nodes, the length of the internodes is affected. An example of this aberrant length can be seen in Figure 3A. Measurement shows that internode length is highly variable, but consistently much shorter than comparable nodes that do form leaves (Figure 2D). It is often the case that only the internode before or after has reduced length, but the overall incidence and magnitude of either is equal.

Midrib Phenotype

One of the consistent leaf morphology defects is the absence of the central stiffening midrib of the leaf blade. This structure normally begins at the ligule/auricle boundary, extending through most of the leaf (Figure 4A). In mutants, many leaves lack this structure entirely along the whole leaf blade (Figures 4B and 4C). This results in characteristic floppy or droopy leaves, often the only observable phenotype in mild mutants. Plastic sections show that the midrib region in midribless leaves lacks the thickening and expanded sclerenchyma of normal leaf midveins (Figures 4D and 4E). Instead, it appears similar to secondary veins that occur laterally along the leaf blade.

In a representative family, midribless leaves occur in roughly 80% of mutants. Plants that display one mutant defect are more likely to have several, with 52% of mutant plants having more than one of midribless or tube leaves in a well-introgressed family in the B73 inbred. These midribless leaves occur along the plant, with most occurring at the 3rd or 4th leaf, but with significant variability (Figure 2E).

Tube Leaf Phenotype

The other major leaf morphology defect is that of fused leaf margins, forming a tubular leaf (Figure 5A). Some leaves, especially juvenile leaves, appear as perfect rings with no indication of a presumptive midrib or margin domain (Figure 5A). Others have expanded sclerenchyma tissue indicative of a midrib domain (Figure 5B). The tube leaf defect occurs at a lower rate than the midribless defect, but in similar positions (Figure 2F). All tube leaves have an open end, demonstrating that the leaf begins forming around the meristem flank as usual. Tube leaves fail to form a cleft separating the leaf margins, instead having growth all around the meristem (Figure 5C and 5D). The tips of tube leaves always display some degree of asymmetry, or in rare cases have two tips much like a pointed bishop's miter (Figure 5I). Transverse sections through these leaves show variable degrees of medial-lateral symmetry. Still others will have a normal leaf blade, while the margins of the sheath are fused (Figure 5J). In either case, abaxial and adaxial tissue is normal (Figure 5H).

In both midribless and tube leaves, the ligule and auricle structures remain unaffected. These tissues divide maize leaves along the proximal-distal axis into the blade and sheath. Even in the most severe cases of altered leaf morphology, the ligule fringe is robustly formed (Figure 5E). Tube leaves make a minimal auricle (Figure 5F). While the auricle generally appears reduced, it always has a degree of asymmetry that bends the leaf.

Inflorescence

The inflorescences of *Hoja loca* mutants have similar defects in lateral organ initiation to the vegetative shoot. In the tassel, there is a reduction in the number of spikelet pairs compared to normal siblings (Figure 6A and 6B). Spikelets are still usually found in pairs, and floral organs lack obvious defects. Tassel branch number is also reduced, as can be in *Hoja loca 2* as it is introgressed into a different inbred background (Figure 2G). The phenotype is not apparent after the first backcross, but subsequent generations begin to show reduced branching. The effects of hybrid vigor may be masking this phenotype in earlier backcrosses. Infertile tassels still extend anthers, but do not shed pollen. Ears have fewer kernels, poorly defined kernel rows, and are reduced in size (Figure 6D).

Roots

No effect in overall root dry mass or lateral root number was observed in *Hoja loca*. 100 two-week old individuals were analyzed in a well-introgressed B73 background. Root dry mass was found to be 3.18g and 3.16g for normal and mutant siblings, respectively, with standard errors below 0.1g. Lateral root numbers were 4.63 and 4.54, with standard errors below 0.15. Obvious differences in root mass are apparent in mature plants, but this difference is very likely attributable to the reduced leaf number and overall reduced growth in severe mutants.

Discussion

The *Hoja loca* mutant phenotype suggests a particular defect in lateral organ initiation. Even severe mutants retain robust phytomeric units, displaying well-formed internodes and even maintaining phyllotaxy despite the absence of leaves. This demonstrates that the basic elements of plant patterning remain functional in *Hoja loca*. Thus, I conclude that the defect must prevent lateral organ initiation after a presumptive organ domain has been established. Indeed, in the case of a single skipped leaf node, the phyllotactic pattern proceeds as though the organ had been made. This extends throughout shoot development, in all cases making mutants appear similar to normal plants that have simply had lateral organs removed.

The morphological defects found in lateral organs are also suggestive of the functional aberration. In mutant leaves, all proximal/distal and adaxial/abaxial patterning remains normal. Sheath, blade, and ligule/auricle are always correctly formed, and the adaxial surface always distinct from the abaxial. However, aspects of medial/lateral patterning are disrupted; midribless leaves lack the medial stiffening domain of leaf blades, and tube leaves lack separation of lateral leaf margins. This is consistent with images of very young leaf primordia that appear as rings about the meristem flank (Figure 5D). A fundamental growth asymmetry from midrib to margin appears to be reduced or lost in cases of morphological defects.

Hoja loca is a unique developmental mutant, but shares some similarities to other maize mutants. Midribless leaves are also observed in *barren inflorescence 2* (*bif2*) mutants and in *drooping leaf* (*drl1,2*) double mutants (McSteen et al. 2007); (Josh Strable, unpublished Dissertation). *bif2* is a knockout of the PINOID homolog, which is a kinase that mediates polar PIN localization, and thus auxin transport (Benjamins et al. 2001). *drl1* and *drl2* are a pair of duplicated YABBY genes that specify the midrib domain. *Hoja loca* and *bif2* are more similar in that they only affect a few leaves on a plant, typically in the early to middle stage of vegetative development. They also both have reduced tassel branch and spikelet formation, though *bif2* lacks a vegetative lateral organ initiation defect. This similarity suggests that auxin transport, or a response to the local auxin maximum at the site of lateral organ initiation, is disrupted in *Hoja loca*.

Genetic analysis of *Hoja loca* supports it being a dominant negative mutation that affects a phenocritical moment in lateral organ initiation. The variable penetrance has no obvious genetic basis as simple selection for a mutant severity does not easily fix that trait. The variation between inbreds demonstrates that the genetic background can affect phenotypic severity, but there must be multiple factors at work. No obvious environmental factor was observed, either. Various families were grown in a variety of conditions in the field and the greenhouse with little effect on the distribution of mutant severity.

Further support for a phenocritical defect comes from observing the patterning of morphological defects. Skipped leaf initiation events, midribless leaves, and tube

leaves all occur stochastically. The only observable pattern is that new periods of growth – during embryogenesis and upon germination – are less likely to produce defects. This is seen as a reduction in aberrations at leaf 1 and also after leaf 7 (Figure 2C).

Finally, while a wide range of severity can be seen, these phenotypes do cluster clearly into severe and mild classes. There appears to be some threshold that, once passed, results in a qualitatively different mode of development.

Materials and Methods

Seed and Growth Conditions: *Hoja loca* was identified in EMS mutagenized seed obtained from Gerry Neuffer. Quantification was performed in families that had been introgressed into the B73 background for at least 3 backcrosses, unless otherwise indicated, and in greenhouse growth conditions. Analysis of *Hoja loca 2* tassel branch number was done in Oxford Tract, Berkeley, CA.

Histology: 10um plastic sections (Figure 4) were made with Technovit® 9100 from Electron Microscopy Services Cat. #14655 according to manufacturer instructions. Sections were mounted on glass slides and stained with toluidine blue. Imaging was performed on a Zeiss Axiovert inverted compound microscope with transmitted light.

Scanning Electron Microscopy: SEMs were performed with material fixed in FAA (3.7% formaldehyde, 50% ethanol, 5% acetic acid) overnight at 4°C and dehydrated in ethanol series to 100%. Sample were critical point dried, sputter coated with palladium, and imaged on a Hitachi S-4700 with 2kV accelerating voltage.

Figures

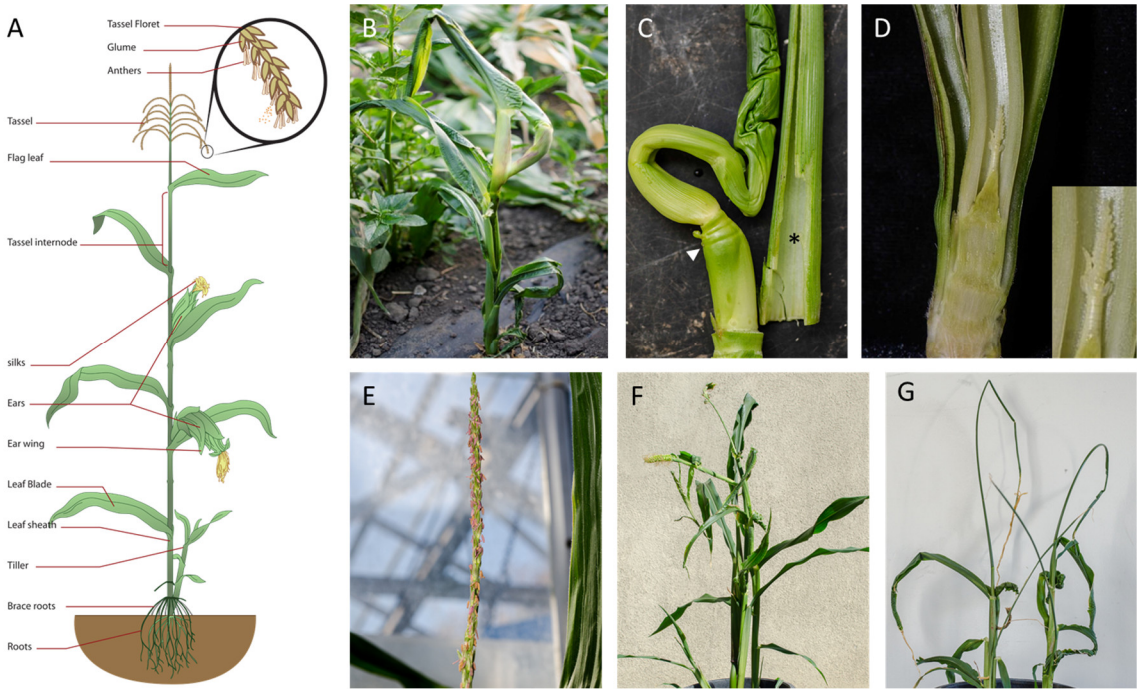

Figure 1: **Maize Morphology and *Hoja loca* Phenotype.** (A) An illustration of the parts of a mature maize plant (Source: https://commons.wikimedia.org/wiki/File:Maize_plant_diagram.svg) (B) A representative *Hoja loca* mutant grown in the field. This is an individual of moderate severity in the B73 background. (C) A cutaway of a mutant with the outer leaf removed (star) showing the trapped inner leaves. An arrow indicates node segments that are lacking leaves. (D) A cross-section of a mutant that has made only two leaves, the inner leaf being a tube leaf. Inset is a magnification of the developing tassel. (E) A mutant tassel in the B73 background showing a lack of tassel branches. (F) A mutant in the W22 background with many tillers and feminized tassels. (G) Two mutants in the A632 background showing tube leaves.

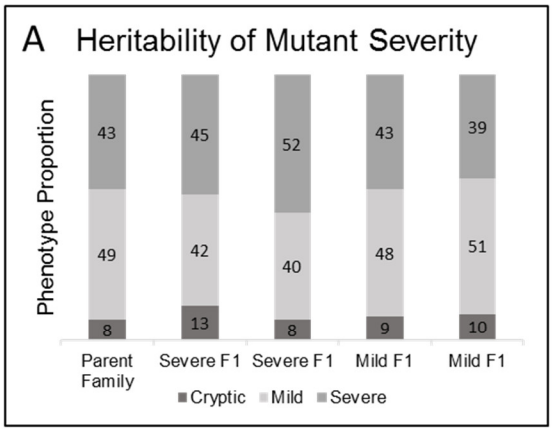
A
Heritability of Mutant Severity
Phenotype Proportion
43
49
8
45
42
13
52
40
8
43
48
9
39
51
10
Parent Family
Severe F1
Severe F1
Mild F1
Mild F1
Cryptic
Mild
Severe

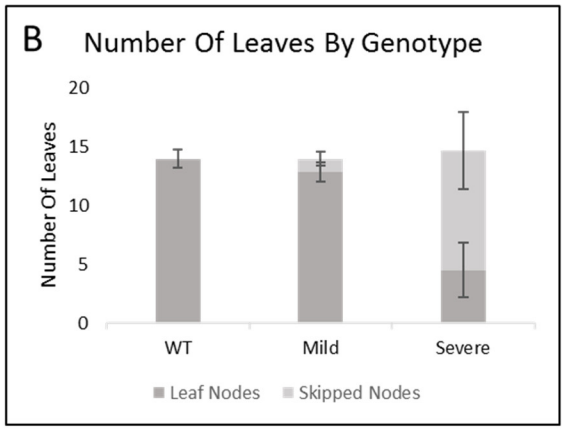
B
Number Of Leaves By Genotype
Number Of Leaves
20
15
10
5
0
WT
Mild
Severe
Leaf Nodes
Skipped Nodes

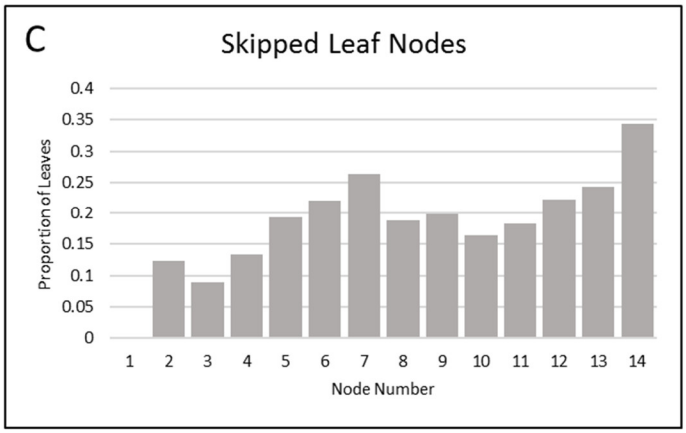
C
Skipped Leaf Nodes
Proportion of Leaves
0.4
0.35
0.3
0.25
0.2
0.15
0.1
0.05
0
1 2 3 4 5 6 7 8 9 10 11 12 13 14
Node Number

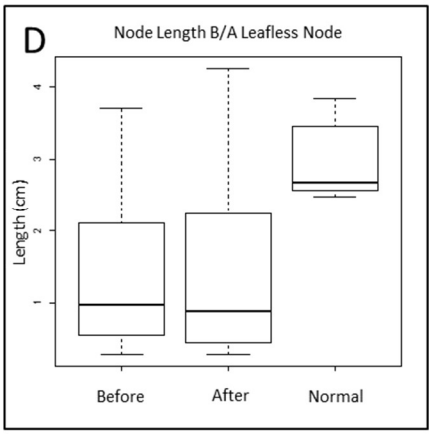
D
Node Length B/A Leafless Node
Length (cm)
Before
After
Normal

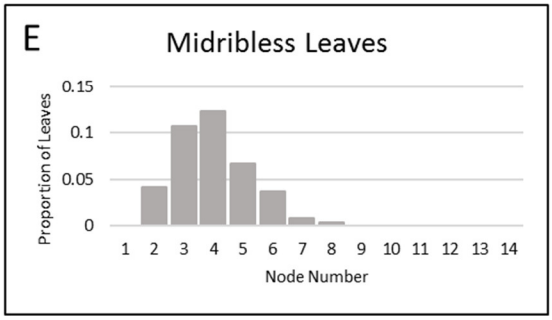
E
Midribless Leaves
Proportion of Leaves
0.15
0.1
0.05
0
1 2 3 4 5 6 7 8 9 10 11 12 13 14
Node Number

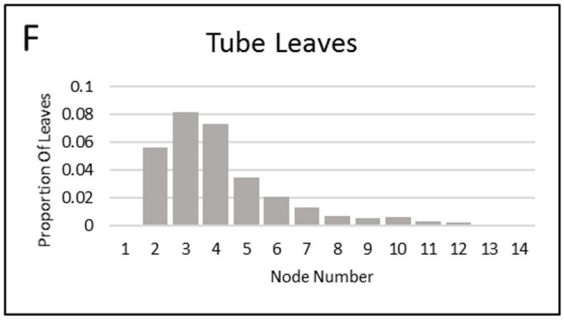
F
Tube Leaves
Proportion Of Leaves
0.1
0.08
0.06
0.04
0.02
0
1 2 3 4 5 6 7 8 9 10 11 12 13 14
Node Number

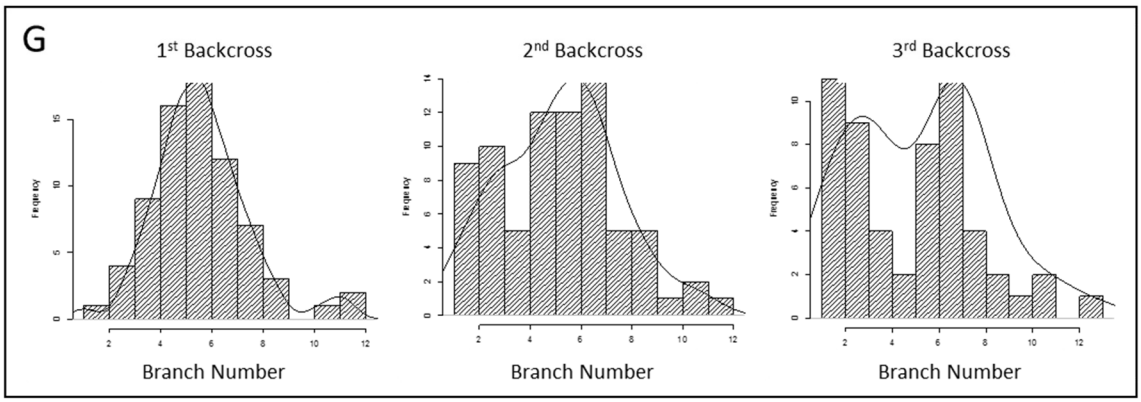
G
1st Backcross
2nd Backcross
3rd Backcross
Branch Number
Branch Number
Branch Number

Figure 2: Quantification of Hoja loca Phenotypes. (A) Analysis of *Hoja loca* mutant severity in families with parents selected for mild or severe phenotypes. The parent family is well introgressed into B73, and the selected individuals are crossed onto B73 ears. At least 150 individuals were analyzed in the resulting families. None of the progeny were significantly different from the parent family by Chi-squared ($p > 0.10$ for all), nor was there as significant bias from selection. (B) Analysis of a representative heterozygous *Hoja loca* family showing leaf counts and presence of skipped nodes. Error bars indicate standard deviation. No significant difference in total node count exists between mutant classes and normal siblings. Scoring severe plants is complicated by the difficulty in distinguishing vegetative and inflorescence nodes, making total node count more variable. (C) Analysis of the location of nodes that lack leaves. The proportion of skipped nodes among mutants in a well-introgressed B73 family is indicated for each position. (D) Analysis of internode length before and after a leafless node compared to comparable nodes in a normal sibling. These plants were grown in a greenhouse at high density, making them shorter than typical maize plants. (E) Analysis of the location of the occurrence of the midribless leaf phenotype, similar to figure C. (F) Analysis of the location of the occurrence of the tube leaf phenotype, similar to panel C. (G) Analysis of tassel branch number as *Hoja loca* 2 is introgressed into the B73 background. The first backcross is similar to wild type with an average of about 6 branches. The second and third backcrosses each reveal more plants with very few or no tassel branches, eventually reaching equal proportion to the normal branch number, as expected in a 1:1 mutant:normal population.

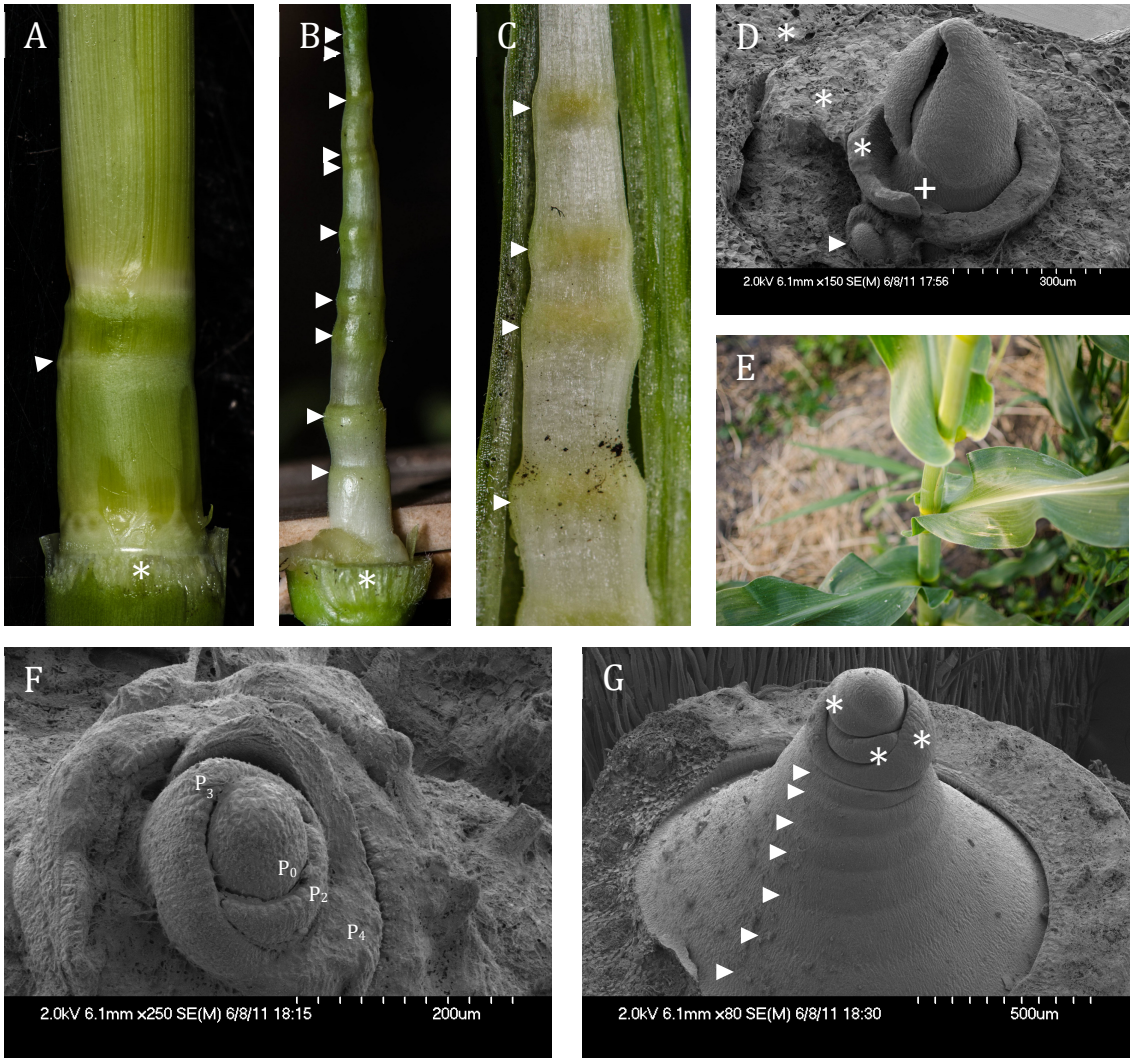

Figure 3: The Skipped Node Phenotype in *Hoja loca*. (A) A mild mutant with one leaf removed (star) to reveal a single skipped node (arrow). (B) A severe mutant with one leaf removed (star) to reveal many successive skipped nodes (arrows). (C) A cross-section of a severe mutant showing tissue differentiation at skipped nodes (arrows). (D) SEM image of a mutant with removed leaves (stars), bare stem segment (cross) and axillary bud (arrow) showing that phyllotaxy is maintained as though skipped nodes had made a leaf. (E) Altered phyllotaxy in a mature plant that is likely due to the shoot being trapped in earlier development. (F) SEM of a non-mutant maize meristem with plastochrons indicated. P_1 is beneath P_3, and leaves from P_4 on have been dissected away. (G) SEM of mutant shoot with outer leaf removed. Seven bare node segments are visible (arrows). Some recovery of leaf formation is seen near the meristem (stars).

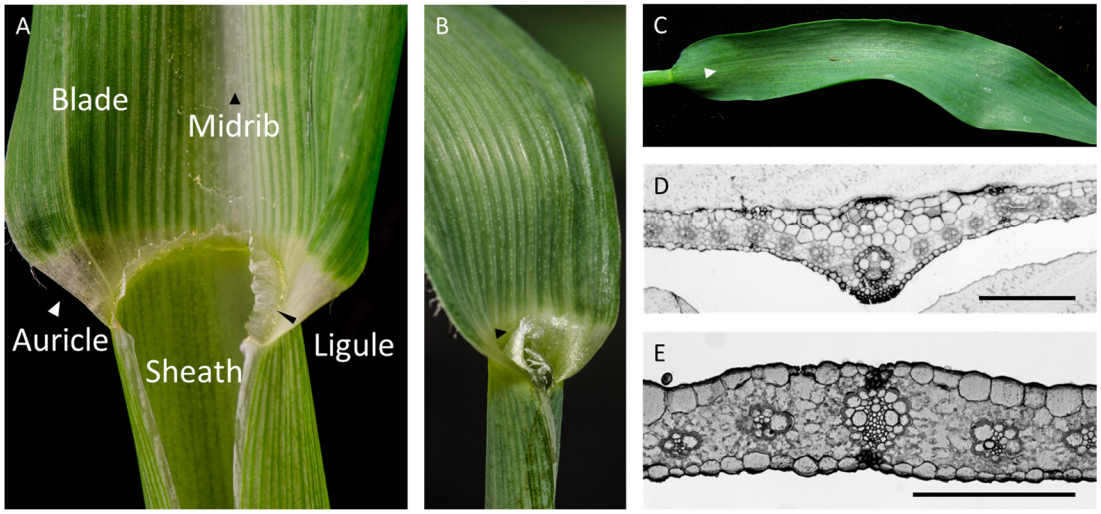

Figure 4: Midribless Leaf Phenotype. (A) WT leaf with various tissues labelled. (B) Hoja loca leaf lacking a midrib with a ligule (arrow). (C) Abaxial leaf surface of midribless leaf, with expected site of midrib (arrow). (D) Plastic section of WT leaf showing midrib. Scale = 1mm (E) Plastic section of Hoja loca leaf showing absence of midrib. Scale = 1mm

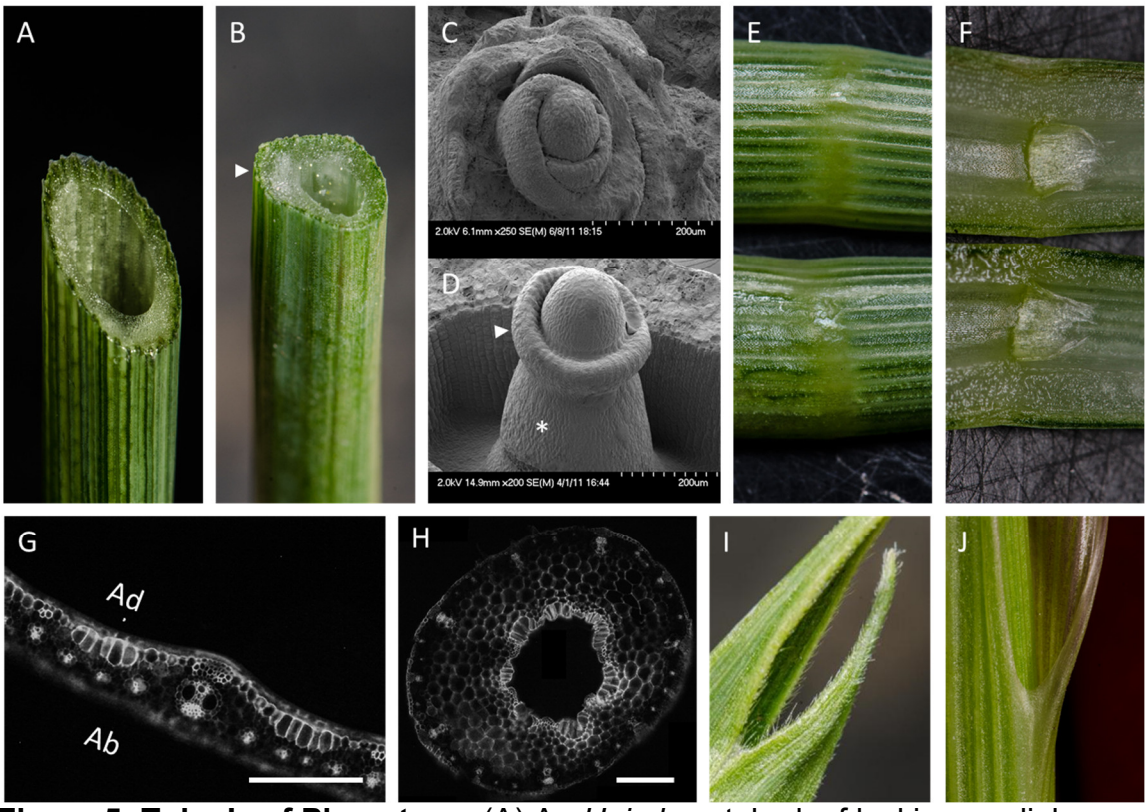

Figure 5: Tube Leaf Phenotype. (A) An *Hoja loca* tube leaf lacking medial-lateral asymmetry. (B) An *Hoja loca* tube leaf with some medial-lateral

asymmetry with a midrib-like structure (arrow). (C) An SEM of a WT SAM. (D) An SEM of a mutant SAM with a bare section of stem (star) and ring-shaped leaf primordium (arrow). (E) A split tube leaf showing the abaxial surfaces of the ligule-auricle junction. (F) A split tube leaf showing the adaxial surfaces, revealing the ligule inside the tube leaf. (G) Fluorescence image of a hand sectioned WT leaf showing the differences in abaxial and adaxial cell types. Scale = 1mm (H) Fluorescence image of a hand sectioned tube leaf with distinct adaxial and abaxial cell types. Scale = 1mm (I) The tip of a tube leaf showing two tips. (J) Leaf margin fusion in the sheath.

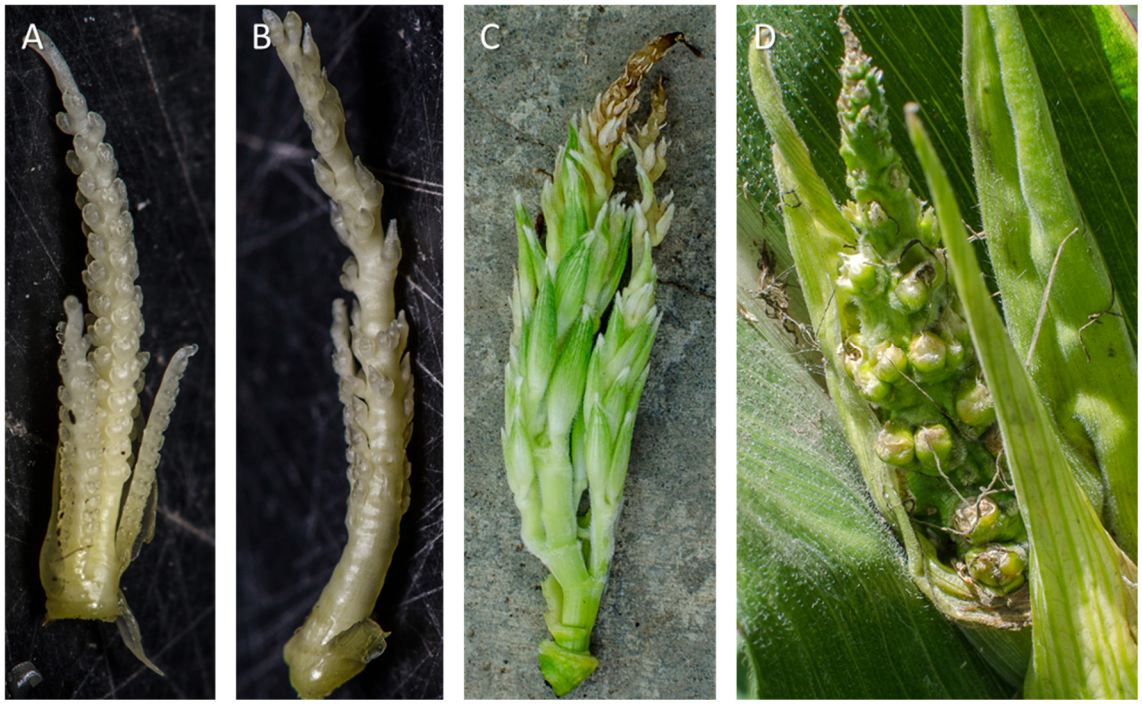

Figure 6: Inflorescence Phenotypes. (A) A young WT tassel. (B) A young *Hoja loca* mutant tassel with sparse spikelet formation. (C) A mutant tassel showing mature outer glumes. (D) An *Hoja loca* ear with malformed kernels.

Chapter 2 – Identifying and quantifying gene expression in *Hoja loca*

Introduction

Having characterized an interesting mutant phenotype, I next sought to identify the mutant locus and causative mutation. The sequencing and assembly of the maize genome allows for positional cloning to be used to identify candidate genes in a chromosomal region (Bortiri, Jackson, and Hake 2006). The markers used for mapping are simple sequence repeats (SSRs), also known as microsatellites. These are common repetitive short sequences of DNA, typically 2 to 4 nucleotides to a repeat, that are prone to mutations in the number of repeats due to DNA polymerase slipping (Morgante and Olivieri 1993). The rate of mutation is such that the different maize inbreds often have variable numbers of repeats relative to one another, yet not so common that changes are unstable

while working with lineages across generations. SSRs have been identified and characterized in a variety of maize inbred backgrounds (Sharopova et al.). This resource permits rapid mapping of maize mutants, provided they have been generated and then introgressed into these backgrounds.

RNA-seq permits high-throughput sequencing of transcriptomes, providing both the cDNA sequence of genes in the mapping interval and characterization of differential gene expression in *Hoja loca*. RNA-seq begins with the formation of a randomly primed cDNA library from RNA fragmented to a target length (Z. Wang, Gerstein, and Snyder 2009). Adapter sequences are added to the ends of these fragments to be compatible with the deep sequencing method used. These tags can include multiplexing sequences that permit many samples to be sequenced in a single lane and computationally separated into different groups (L. Wang et al. 2011). The generated reads are then mapped to a genome using a reference of known splice sites (Wu and Watanabe 2005; Wu and Nacu 2010). The mapped reads can be directly investigated to observe single nucleotide polymorphisms (SNPs) and splicing variants. Differential gene expression can be calculated computationally by analyzing the Fragments Per Kilobase of transcript per Million mapped reads (FPKM) (Trapnell et al. 2010).

Results

Mapping

Positional cloning was performed on *Hoja loca* introgressed into A619 for rough mapping and B73 for the final walk to the candidate interval. Difficulties in scoring the mutant phenotype necessitated the use of only mutants in mapping, as cryptic phenotypes make wild type plants unreliable. Custom SSR markers were developed to narrow the interval beyond what was available from stock centers. The mapping results are presented in Table 1, yielding a candidate interval on Chromosome 8 between 109.7 and 110.6 megabases. There are 18 annotated loci in this interval, 12 of which are considered unknown or weakly homologous to known genes.

At the time of mapping to this interval, the 3rd version of the maize genome had only recently been released, and many annotations had not yet been updated. Sequencing efforts concentrated on GRMZM2G101852, a homolog of the Seven In Absentia (SINA) protein originally described in *Drosophila melanogaster*. This gene is an E3 ligase involved in protein ubiquitination. In *Arabidopsis thaliana*, SINAT5 was identified as an interactor with the NAC1 transcriptional activator, part of the auxin signaling transduction network (Qi Xie et al. 2002; Q Xie et al. 2000). Overexpression of SINAT5 resulted in plants that failed to initiate lateral roots, while a dominant negative version of the protein developed more lateral roots. This link to lateral organ initiation prompted investigation into the maize homolog in the candidate interval.

Sanger sequencing was performed on GRMZM2G101852 and 5 other candidates based on their annotations. cDNA and genomic DNA were both used

with primers designed to cover exon and coding sequence for all candidates. Heterozygous material was used because of the difficulty in generating homozygotes from well-introgressed material. GRMZM2G101852 was completely sequenced from the promoter to the 3' UTR. While several polymorphisms between the inbred backgrounds were found, none were unique to the mutant.

RNAseq Analysis

RNAseq was performed to both characterize gene expression in the mutants and to efficiently sequence transcribed regions of the candidate region. A well-introgressed *Hoja loca* family in the B73 background was used. Three samples of 10 shoot apices were selected for both mutant and normal siblings. Genotype was assessed with SSRs flanking the candidate region. Shoot material including the SAM and some young leaves was collected from plants 14 days after germination. This age was chosen to ensure that changes in gene expression would be present but not too severe. At this point, approximately half of the mutant plants had no visible defects, 40% had mild defects including midribless leaves, and the remaining 10% were severe plants with a visible deficiency in leaf initiation. Selecting this younger material should ensure that secondary effects such as plant stress won't overwhelm any primary transcriptional responses.

Each RNAseq library ranged from 9 to 13 million uniquely mapped reads. The percentage of uniquely mapping reads varied from 50% to 60%, which is typical for 50bp reads in maize. RNAseq results for select genes were confirmed with quantitative real time PCR (qPCR). Changes in gene expression for PIN1a, SoPIN, KN1, and GLU1 were quantified and agree with the RNAseq results. PIN1a was downregulated to 0.72 +/- 0.12 fold of normal sibling expression by qPCR, and 0.86 by RNAseq. SoPIN was downregulated to 0.81 +/- 0.07 fold of normal sibling expression by qPCR, and 0.73 by RNAseq. KN1 was upregulated to 1.22 +/- 0.18 fold of normal sibling expression by qPCR, and 1.34 by RNAseq. GLU1 was upregulated to 49 +/- 7.3 fold of normal sibling expression by qPCR, and 60.3 by RNAseq.

Analyzing the RNAseq data began with a manual search for candidate SNPs in the mapped region. This search was performed with Integrative Genome Viewer (https://www.broadinstitute.org/igv/) which visually displays polymorphisms on individual reads. Polymorphisms were investigated if they occurred in roughly half of the mutant reads. Other proportions are likely PCR-amplified errors. Known Mo17 polymorphisms were collected from HapMapV3 from Panzea (https://hapmap.ncbi.nlm.nih.gov/) to eliminate known polymorphisms between the inbreds. SNPs that were not a G to A or C to T were also rejected as the mutation was generated with EMS (Griffiths et al. 2000). Of the 18 candidate loci, only one SNP occurred in a coding region that satisfied these criteria. This was a C to T nucleotide transition at position 110,340,849 on chromosome 8. This coding region corresponds to GRMZM2G035465.

GRMZM2G035465 is currently annotated as ZmIAA38 on www.maizegdb.org as of the publication of this thesis, one of 44 annotated IAA genes in maize. It has also been annotated as ZmIAA28 (Ludwig, Zhang, and Hochholdinger 2013). The genome assembly for this gene changed between the first and third version of the maize genomes, resulting in no annotation being present in common annotation lists until relatively recently.

ZmIAA38 is a canonical *AUXIN/INDOLE-3-ACETIC ACID* (Aux/IAA) gene 216 amino acids long with all four classic protein domains. Aux/IAA genes are unique to plants, with most being responsive to exogenous auxin treatment (Reed 2001). These proteins are nuclear localized and experience rapid turnover (Abel, Oeller, and Theologis 1994). They contain four domains: domain I is an active repression domain, domain II mediates protein stability, and domains III and IV permit homo- and hetero-dimerization with both other Aux/IAA members and ARF proteins (Tiwari, Hagen, and Guilfoyle 2004; Worley et al. 2000; Ouellet, Overvoorde, and Theologis 2001).

Members of the Aux/IAA family display extensive functional redundancy. Even triple mutants have little discernable phenotype; instead, dominant gain-of-function mutants are useful for analyzing their function (Overvoorde et al. 2005). Domain II Aux/IAA mutants are dominant or semi-dominant and have a variety of developmental defects affecting leaf formation and expansion, apical dominance, lateral root formation, and root and shoot gravitropism (Reed 2001).

The C to T transition in *Hoja loca* causes a missense mutation at amino acid position 108 from a Glycine to Glutamic Acid. Glycine is a small, non-polar residue whereas Glutamic Acid is a large acid residue, making this change significant. This position is in the center of the highly-conserved Domain II of Aux/IAAs in a sequence known as the degron, specifically the very highly conserved Gly-Trp-Pro-Pro-Val (GWPPV) motif. In Arabidopsis, at least fifteen dominant Aux/IAA mutant alleles have been reported in nine Aux/IAA genes (Reed 2001). Of these, three alleles are missense mutations at the Glycine in the degron sequence, and two of them – *shy2-3* and *iaa18-1* – are mutations to code for a Glutamic Acid. All of these mutations cause developmental defects related to auxin signaling. This makes it very likely that *Hoja loca* is a dominant gain-of-function mutation in ZmIAA38 that results in a stable protein insensitive to auxin signaling. This missense mutation is the only one in the mapping interval, and the mutant phenotype is consistent with other Aux/IAA dominant or semi-dominant phenotypes.

The Arabidopsis homolog of ZmIAA38 is AtIAA27 (AT4G29080) according to the MaizeGDB (http://www.maizegdb.org/gene_center/gene/GRMZM2G035465) annotation and confirmed by BLAST (https://blast.ncbi.nlm.nih.gov/Blast.cgi) search. AT4G29080 is also called Phytochrome Associated Protein 2 (PAP2) – not to be confused with the MYB transcription factor phosphatidic acid

phosphatase 2 also called PAP2 – based on the results of a yeast two hybrid (Y2H) screen (Choi et al. 1999). Other Aux/IAA genes, such as SHY2/IAA3, are known to be regulated by light, suggesting a link between light and auxin signaling (Tian, Uhlir, and Reed 2002).

No mutants of AtIAA27 have been studied, but the gene is identified in several publications related to toxic stress and infection. AtIAA27 was the second most upregulated genes in response to naphthalene treatment [Peng et al., 2011]. Naphthalene is closely related to 1-Naphthaleneacetic acid (NAA), a synthetic auxin often used in horticulture and plant tissue culture, and several auxin related genes appear in the gene list. It is also differentially expressed in studies investigating polycyclic aromatic hydrocarbons, phenols, and toluene (Alkio et al. 2005; Xu et al. 2012; Gao et al. 2012). Finally, AtIAA27 was investigated in the context of *Tobacco mosaic virus* (TMV) infection (Padmanabhan, Shiferaw, and Culver 2006). Both AtIAA27/PAP2 and the related AtIAA26/PAP1 interact with the TMV replicase protein upon infection. This interaction mediates a change in subcellular localization of the two IAAs from nuclear to cytoplasmic inclusions known as vesicle-like replicase complexes. This finding suggests that TMV infection affects auxin signaling via these Aux/IAA proteins. Notably, IAA27:GUS reporter activity was observed at the site of lateral root initiation (Collum et al. 2016).

***Hoja loca* 2**

The putative second allele of *Hoja loca* was mapped between SSR markers phi100175 and umc1858, giving a mapping interval on chromosome 8 from 101-113 megabases, a region that covers the *Hoja loca* locus at 110.3 megabases. Sanger sequencing of *Hoja loca 2* cDNA reveals a G to A transition in the second exon that results in a Glutamic Acid to Lysine mutation outside the domain II region. This residue is not as highly conserved as the *Hoja loca* mutation, but that may be consistent with the milder phenotype.

Differential Gene Expression

Comparing RNAseq reads between mutant and normal sibling samples enables analysis of differential gene expression in the mutant. Cuffdiff was used to generate a list of significantly differentially expressed genes using the default settings (Trapnell et al. 2010) (Table 2). This is a concise list of 58 genes, indicating that the staging of plants and material used was appropriate for finding primary effects of the *Hoja loca* mutation.

Selected genes are discussed below. Genes that aren't included either lack sufficient homology to suggest gene function or are insufficiently differentially expressed to discuss.

GRMZM2G034152 encodes POLYAMINE OXIDASE 1 (PAO) and is upregulated 42 fold in *Hoja loca*. ZmPAO is known to oxidize spermidine and spermine, compounds which are known to cause short shoots and dark green leaves

(Fiorillo et al. 2011; Tassoni et al. 2000). Dark green leaves are observed in severe *Hoja loca* mutants, but this is not an expected effect of an upregulated spermidine oxidizer which would reduce spermidine levels. This gene has also been implicated in leaf elongation under saline stress and abscisic acid-induced cytosolic antioxidant defense in leaves (Rodríguez et al. 2009; Xue, Zhang, and Jiang 2009).

GRMZM2G050875 is upregulated 39 fold and has weak homology to XM_004958535, a *Seteria italica* protein annotated as EARLY RESPONSE TO DEHYDRATION 15-like. ERD15 is an *Arabidopsis* protein that is known to be a negative regulator of Abscisic Acid response (Kariola et al. 2006).

GRMZM2G033544 is upregulated 32 fold and is likely to encode a homolog of a cyclopropane-fatty-acyl-phospholipid synthase. This gene is responsible for a fatty acid synthesis, but little is known about the physiological effects it might have in plants. It is also lowly expressed on an absolute scale, with the gene only mapping a few reads in the normal sibling sample.

GRMZM2G101958 encodes PHOSPHOLIPID TRANSFER PROTEIN 1 (PLT1) and is upregulated 24 fold. Lipid transfer proteins transfer phospholipids between membranes and likely are involved in membrane biogenesis [Kader 1996]. They are also secreted into the cell wall, possibly functioning in environmental adaptations or pathogen defense.

GRMZM2G057258 is upregulated 13 fold and is annotated as an acid phosphatase/vanadium-dependent haloperoxidase related protein.

GRMZM2G021573 and GRMZM2G028151 both encode AP2-EREBP transcription factors related to the AINTEGUMENTA (ANT) protein in *Arabidopsis*, and both are expressed one third as much in mutants. ANT regulates growth and cell number in shoot organogenesis by maintaining meristematic competence (Mizukami and Fischer 2000).

GRMZM2G156861 encodes LIPOXYGENASE 1 and is upregulated 4 fold. This gene is known to be induced by pathogens and abscisic acid in *Arabidopsis* (Melan et al. 1993).

GRMZM5G879665 encodes a cytokinin riboside related to the LONELY GUY1 (LOG1) gene in rice and is downregulated to one quarter of normal sibling expression. LONELY GUY1 is a cytokinin activating protein required for shoot meristem maintenance (Kurakawa et al. 2007).

GRMZM2G079013 encodes a LEUNIG_HOMOLOG gene that is downregulated to one fifth of normal sibling expression. This gene is known in *Arabidopsis* to be part of a transcriptional repressor complex with YABBY domain proteins. These

genes promote adaxial cell identity and are important in maintaining leaf polarity and meristem activity (Stahle et al. 2009).

GRMZM2G008792 encodes the cytokinin oxidase CKX12 and is downregulated to one fifth of normal sibling expression. Cytokinin oxidases degrade cytokinin and a protein of this family has been shown to affect tiller number in rice (Yeh et al. 2015).

GRMZM2G328005 is downregulated to one tenth of normal sib expression. It has no gene annotation, but is homologous to a segment of anthocyanidin 3-O-glucosyltransferase: NM_001153796. This BLAST his suggests it could have glucosyltransferase activity. However, the opposite strand contains the GRMZM5G822479 gene model and is annotated as a transposon.

GRMZM2G047588 is the most downregulated gene at one twenty-fifth of normal sibling expression. It encodes an uncharacterized protein kinase superfamily protein (APK1A). It has homology with the *Arabidopsis* protein BOTRYTIS-INDUCED KINASE1 (BIK1) which regulates immune responses and ethylene signaling (Laluk et al. 2011).

GRMZM2G016890 is the most upregulated gene at a 60-fold change in expression. It encodes BETA GULCOSIDASE 1 (ZmGLU1), a member of a family of enzymes that cleave glucose conjugates from molecules such as plant hormones like cytokinin (CK), abscisic acid (ABA), lignin, myrosinase, and scopolin (Brzobohatý et al. 1993; K. H. Lee et al. 2006; Escamilla-Treviño et al. 2006). The removal of the glucose molecule generally facilitates rapid activation of chemical signals, or lignin biosynthesis in the case of monolignol glucoside hydrolysis. GLU1 contains a full auxin responsive element (AuxRE - TGTCTC) 83 base pairs upstream of the transcription start site, as well as several TGTC sequences within 1kb upstream.

ZmGLU1 was first identified as Zm-p60 by looking for auxin-binding proteins from maize extracts (Campos et al. 1992). This protein was identified as a beta-glucosidase and biochemically characterized to hydrolyze a variety of O-linked glucosides. Further work sequenced this protein and showed it to be an *in vivo* activator of Cytokinin (Brzobohatý et al. 1993). The sequence positively identifies the protein as a GRMZM2G016890 product. Zm-p60 was tested against a variety of compounds for hydrolase activity, noting that cellobiose, salicin, rutin, and IAA-glucose-ester were all unaffected, though IAA-glucose-ester is able to inhibit hydrolase activity. Cytokinin O-glucosides – the common conjugate found in plants opposed to N-glucosides – were hydrolyzed to active Cytokinin in tobacco mesophyll protoplasts. Transformed calli were able to grow with zeatin-O-glucoside (ZOG) for many months, indicating that ZOG was being made into active cytokinin in a Zm-p60 dependent manner. Immunocytochemical staining showed that Zm-p60 is located in zones of active cell division in roots.

This is consistent with the maize embryo activating phytohormone conjugates from the endosperm to maintain meristem activity.

Further work showed that Zm-p60 is targeted to plastids and is present in a variety of tissues by immunolocalization (Kristoffersen et al. 2000). Notably, it is present in the vascular bundles of the coleoptile and in the outermost cell layer and the vascular tissue in leaves. Finally, Zm-p60.1 was overexpressed in tobacco, showing reduced root growth and ectopic growth near hypocotyls in the presence of zeatin (Kiran et al. 2006).

The closest *Arabidopsis* homolog is AT2G44450 or AtBGLU15 which has been characterized in detail by (Roepke and Bozzo 2015). This gene belongs to a subclade of Glucosidase proteins consisting of BGLU12 (At5g42260), BGLU13 (At5g44640), BGLU14 (At2g25630), BGLU15 (At2g44450), BGLU16 (At3g60130), and BGLU17 (At2g44480). This clade is distant from the aforementioned glucosidase members, being instead more related to isoflavone BGLUs. BGLU15 was studied in the context of nitrogen deficiency and low temperature stress (NDLT). NDLT in Arabidopsis results in accumulation of flavonol bisglycosides, namely K3G7R and Q3G7R. These levels return to normal when plants are put into conditions of nitrogen sufficiency and high temperature (NSHT). Gene expression profiling showed that BGLU15 was highly upregulated upon return to normal conditions, suggesting that it could be responsible for degrading these flavonol bisglycosides. Biochemical work confirmed that BGLU15 is highly specific for 3-O- B-glucosides, and had highest activity on flavonol bisglucosides, especially K3G7R.

An interesting line of evidence supporting the involvement of ZmGLU1 in organogenesis comes from expression profiling of the ligule (Johnston et al. 2014). Using laser capture microdissection, an expression profile of the preligule region vs. sheath and blade tissue was generated. ZmGLU1 was the second most upregulated gene in the ligule relative to the sheath, and also highly upregulated relative to the blade. It was also the 9th most downregulated gene in *liguleless1 (lg1)* mutants that lack a ligule. A role for ZmGLU1 in organogenesis is further supported by data obtained from a laser capture microdissection study. Four adjacent zones of a plastochron 4 leaf primordia were captured starting with a region attached to the leaf and moving distally. ZmGLU1 expression is absent from most zones, but highly expressed in a boundary zone, an area that may predict early events leading to the ligule [M Scanlon, personal communication].

Discussion

Hoja loca has been identified as a mutation of ZmIAA38. Mapping of two independent alleles leads to this chromosomal region containing only a few genes that appear to be functional. Using the aligned RNAseq reads, I found only one polymorphism in this region that could be caused by EMS. Furthermore, the *Hoja loca* phenotype is consistent with described *Aux/IAA* mutants; the allele behaves dominantly and has a variety of effects on plant

development. The resulting amino acid change is identical to two other described Aux/IAA mutants, showing that the mutation in question is capable of affecting Aux/IAA function. Finally, the second allele also has a mutation in this gene. Together, these data support *Hoja loca* as a protein stabilizing mutation in domain II of ZmIAA38.

ZmIAA38 has not been investigated in detail before, nor the AtIAA27 homolog. Studies of the entire Aux/IAA family show that AtIAA27 is not exceptional, behaving similarly to other members in protein interactions and similar in protein structure [Piya et al. 2014, Wang et al. 2014]. Extrapolations about ZmIAA38 function are further complicated by the uncertainty and complexity in Aux/IAA interactions with ARFs. While the classic auxin signal transduction involves IAA degradation and subsequent release of the ARF binding partner to activate gene transcription, there are also possibilities for more binding complexity, binding competition, and chromatin modification (R. Wang and Estelle 2014).

Suggestions for Hoja loca function come from looking at differential gene expression in the mutant. This short gene list contains a variety of loci, many of which have no homology to other genes in maize or other species. Of those that have described homologs, few are suggestive of having a functional consequence consistent with the mutant phenotype. GRMZM2G050875 and GRMZM2G034152 are both related to ABA signaling, but one would promote it, and the other reduce it. There is also GRMZM2G079013, a potential YABBY interactor in the abaxial leaf domain and promotor of adaxial cell fate. This could conceivably be a consequence or cause of the leaf morphology defects in *Hoja loca*. GRMZM2G021573 and GRMZM2G028151 are both related to ANT and downregulated in the mutant, suggesting that these genes could promote organogenesis.

At least three differentially expressed genes are related to cytokinin. GRMZM2G008792 is a cytokinin oxidase that degrades cytokinin. A related gene was shown to affect tiller development in rice, suggesting that this gene may be involved in organ growth (Yeh et al. 2015). There is also GRMZM5G879665 which encodes a cytokinin riboside related to LONELY GUY (LOG). LOG is required for meristem maintenance, whereas *Hoja loca* has no early meristem termination phenotype, but other LOG family proteins have diverse effects in embryogenesis, leaf vascular tissues, apical dominance, and leaf senescence (Kuroha et al. 2009). The differential expression of these genes could cause altered cytokinin signaling, or perhaps reflect altered cytokinin signaling and feedback in mutant shoots.

The most promising link to a possible explanation for the mutant defect comes from GRMZM2G016890. This beta glucosidase is responsible for activating cytokinin and is expressed in a variety of plant tissues. Cytokinin and auxin are both important for meristem development, and often act antagonistically (Su, Liu, and Zhang 2011). Additionally, cytokinin is required for robust phyllotactic

patterning in *Arabidopsis* shoots (Besnard et al. 2014). Since *Hoja loca* overexpresses this gene, it would follow that there could be ectopic cytokinin activation in the mutant, thus affecting the balance of auxin and cytokinin. This disruption could lead to failure to initiate lateral organs.

ZmGLU1 also has very close homology to a well-described Arabidopsis homolog that specifically degrades bisglucoside flavonols. Flavonols have been implicated in a variety of auxin signaling and patterning processes including lateral root organogenesis (Grunewald et al. 2012). Flavonols, specifically the early biosynthetic intermediate naringenin, are known to inhibit auxin transport when exogenously applied to plants (Brown et al. 2001). This suggests the possibility that auxin signaling could regulate flavonol accumulation in the shoot, and thus feedback into auxin patterning.

Regardless of ZmGLU1 function in the maize shoot and its effect on auxin transport, the ligule expression profiling shows that ZmGLU1 is an attractive target for investigation (Johnston et al. 2014). This data constitutes an independent line of evidence that ZmGLU1 is involved in organogenesis. Ligule formation is highly analogous to leaf and branch initiation, and indeed this was the main conclusion from the study. Both events involve the formation of a local auxin maximum and subsequent organ outgrowth. However, *Hoja loca* and *liguleless1* mutants fail to form their respective organs, but their expression of ZmGLU1 is opposite. Reconciling this difference will be critical for understanding the function of ZmGLU1 during organogenesis.

Methods

RNAseq: RNA was extracted from 14 day old shoot apices consisting of cylinder of tissue approximately 2mm in diameter and 5mm in length, centered on the SAM. Total RNA extraction was done with Trizol (Invitrogen). Poly-A RNA was purified from 2ug of total RNA using a Dynabeads Oligo(dT) kit (Invitrogen) and repeated to eliminate rRNA. RNA-seq libraries were prepared using the ScriptSeq v2 RNA-Seq library preparation kit (Epicentre) based on the manufacturer's protocol. 6 libraries consisting of 10 individuals each, 3 mutant and 3 normal sibling, were indexed using ScriptSeq Index PCR primers (Epicenter), pooled, and sequenced using 50bp single-end reads on Illumina Hisequation 2000.

RNAseq Analysis: Reads were aligned to the reference maize genome (http://ensemblgenomes.org/ release 28) using GSNAP v.10.7 (http://research-pub.gene.com/gmap/) with guide annotation. Differential gene expression was calculated with cuffdiff from the Cufflinks package (v.2.0.2) (Trapnell et al. 2010).

RT-qPCR Analysis: RNA was extracted using Trizol and purified from 1 µg of total RNA using Dynabeads oligo(dT) (Invitrogen). cDNA was synthesized as described previously (Tsuda et al. 2011). Purified mRNA was reverse transcribed by Superscript III reverse transcriptase (Invitrogen), and 1uL of 1:5

diluted cDNA was used for a 20uL qPCR reaction as described previously [Bolduc et al., 2009]. Samples were normalized with GAPDH expression. Primers used are: GLU1 forward – ACTGGACGGGAGCAATTCAG, GLU1 reverse – TTCTTTGGTTCCCTTCGGCA; PIN1a forward – ACGGCGTGCACCCTGACATC, PIN1a reverse – GCTGCCCATCACGCTGGTGT; KN1 forward – GGCCACAGACAAACTGTTGA, KN1 reverse – GAAAGAGTGCATGCAACCAA; GAPDH forward – CCTGCTTCTCATGGATGGTT, GAPDH reverse – TGGTAGCAGGAAGGGAAACA.

Tables

SSR Name	umc1157	umc1457	IDP8545	IDP8407	DX	EK	SINA	DT	DJ	umc1858	TIDP4637	BY	CH	CA	CF	BNLG1176	AO	AD	UMC 1846
Megabases	70.53	101.53	105.03	106.53	109.23	109.745	109.9	110.52	110.67	112.06	114.7	116.83	117.43	117.92	118.53	120.47	122.0003	124.643	130.27
f19	1	2								2								2	
f38	1	2								2									
f9	1	2								2								2	
f15	1	1	2	2						2							2	2	2
f28	1	1	1	1						2							2		2
i11				1	2	2		2	2		2	1							
k13				1	2	2			2										
g32				1	2	2	2	2	2			2							
j23					2	2	2	2	2		2	2							
f28				1	1	1	2	2	2			2							
g28				1	1	1	2	2	2			2							
h10					2	2		2	1		1	1							
k40				2	2	2			2		1								
i7									2		2	1							
j10											2	1							
g4										2	2	2	2	1	1	1	1		1
h14			2							2	2	2	2	2	2	1	1		1
g32										2	2	2	2	2	2	1	1		1
f7	2	2	2	2						2							2	1	1
g5										2							2		1
g9										2							2		1
g11										2							2		1
g26										2							2		1
118-6			2							2							2		1

Table1 – Mapping *Hoja loca*: SSR marker sequences were obtained from MaizeGDB (http://www.maizegdb.org/) that could distinguish between Mo17 and B73. Further markers were designed with Gramene's SSRIT tool (http://archive.gramene.org/db/markers/ssrtool) and validated with NCBI's Primer Blast (https://www.ncbi.nlm.nih.gov/tools/primer-blast/). These custom SSRs are given two-letter names. Finally, sequence polymorphisms in the SINA gene were used as markers by Sanger sequencing. A selection of recombinant plants with clear mutant phenotypes and SSRs is shown. The numbers in the cells indicate the number of SSR variants observed by gel electrophoresis; two bands indicate heterozygous material that retains the Mo17 sequence, while one band is homozygous for B73 variants and thus excludes that region from the candidate interval. Cells with no number indicated are shaded according to the inferred genotype at that location.

Name	Chromosome:Location	Normal Sib Reads	Mutant Sib Reads	q-value	Fold Change	Description
GRMZM2G047588	8:133596702-133607955	129.23	5.5283	0.017163	0.010599	APK1a Protein kinase superfamily protein
GRMZM2G328005	3:71569068-71570793	18.448	3.5442	0.029646	0.092553	Possible glucosyl-transferase
NDHD	Pt:91652-131084	30.441	7.3718	0.017163	0.129263	NADH Dehydrogenase subunit D
GRMZM2G095114	8:5029915-5039269	1756	467.96	0.029646	0.148408	Small ribonuclear protein
GRMZM2G079013	5:215387950-215401364	433.77	117.93	0.042767	0.152731	LUH gprotein, wd40
GRMZM6G787651	7:173847829-173853197	15.886	4.3603	0.042767	0.154861	CDF3 - Cycling DOF factor 3
GRMZM2G120918	5:159796627-159797566	135.34	39.295	0.017163	0.167933	ChaC-like family protein
AC212467.3_FG001	5:87963083-87963389	999.36	307.68	0.017163	0.182762	Probable transposon
PSBC	Pt:6391-15097	51.698	16.163	0.042767	0.186861	Photosystem II CP-43 protein
GRMZM2G008792	2:28171678-28176605	84.053	27.047	0.017163	0.194793	CKX12 - Cytokinin oxidase 12
GRMZM2G163471	2:37953939-37960212	70.445	23.478	0.017163	0.204901	eukaryotic translation initiation factor 4B1
GRMZM2G114055	1:21756542-21775704	136.56	47.428	0.017163	0.217464	(NPY2) Phototropic-responsive NPH3 family protein
GRMZM2G069911	9:23826466-23827831	41.601	14.818	0.036917	0.225526	(HIS1-3) histone H1-3
AC208724.3_FG001	4:230752308-230755184	457.6	164.63	0.017163	0.228815	Unknown
GRMZM2G069525	2:17494662-17498413	63.539	22.982	0.017163	0.230584	GLK37 - G2-like transcription factor
RPS16	Pt:3362-5604	28.794	10.645	0.036917	0.23797	Chloroplast Ribosomal Protein S16
AC209835.4_FG004	5:21903402-21908619	105.5	39.853	0.017163	0.245509	ChaC-like family protein
GRMZM2G155232	8:15110788-15113681	64.022	24.316	0.017163	0.247424	Serine carboxypeptidase-like
GRMZM2G150256	6:89066266-89071191	43.559	16.695	0.029646	0.25068	MIR2 - Maize Insect Resistance2, protease
GRMZM2G114775	1:295848927-295850422	123.8	48.057	0.017163	0.25534	GATA18 - C2C2-GATA-Transcription Factor 18
GRMZM2G025024	2:149351722-149356144	20.797	8.0985	0.036917	0.256502	Protein kinase superfamily protein
GRMZM2G373522	4:154337341-154339063	119.35	46.751	0.036917	0.258686	Dehydrin putative expressed
GRMZM2G123896	1:222643513-222645307	239.32	94.543	0.017163	0.261869	DRM1 - Dormancy Associated 1
GRMZM2G051491	2:152242068-152244277	62.148	24.658	0.017163	0.263514	Methyl esterase
GRMZM2G014844	10:34733948-34737952	628.98	257.6	0.036917	0.275849	GLU3 - Beta-glucosidase 3
GRMZM5G879665	1:230982815-230985511	90.338	37.085	0.017163	0.276792	Cytokinin Riboside - LOG1 homolog
GRMZM2G023313	1:182129145-182131165	328.25	139.08	0.029646	0.28972	Unknown Expressed Protein
AC187891.3_FG006	10:6406677-6407469	80.66	34.232	0.042767	0.290402	OFP39 - OVATE-Transcription Factor 39
GRMZM2G180246	1:273393235-273396891	494.48	210.23	0.017163	0.29114	GIF1 - Growth-Regulating-Factor-Interacting Factor 1
GRMZM2G341036	5:27150768-27152027	90.734	38.583	0.036917	0.291219	Unknown Expressed Protein
GRMZM2G077744	2:2343331-2351035	72.502	30.993	0.029646	0.293441	Possible signal recognition particle 19 kDa protein
GRMZM2G021674	6:359786-364379	27.96	12.339	0.017163	0.307251	Possible single-stranded DNA endonuclease family protein
GRMZM2G023291	1:251772747-251774599	83.235	37.151	0.036917	0.312297	HB124 - Homeobox Transcription Factor 124
GRMZM2G021573	9:145136033-145140341	83.027	37.157	0.042767	0.313499	EREB161 - AP2-EREBP Transcription Factor 161
GRMZM2G050484	4:233803554-233809152	33.916	15.189	0.017163	0.313812	ZLP1 - ZIP-like Protein 1, zinc transporter
GRMZM2G028151	1:281700005-281703981	101.48	45.494	0.017163	0.314293	EREB184 - AP2-EREBP Transcription Factor 184
GRMZM2G038284	6:164572346-164575688	96.911	46.176	0.029646	0.34317	Drought-responsive family protein
H4C14	8:117349861-117351374	150.57	311.99	0.017163	2.860596	Histone H4C14
GRMZM2G176307	5:181570932-181575725	29.772	63.446	0.036917	2.978977	GPC4 - Glyceraldehyde-3-phosphate dehydrogenase4
GRMZM2G011523	3:23906022-24097603	373.73	834.64	0.017163	3.187191	Related to BBTI11 - Bowman-Birk type bran trypsin inhibitor
GRMZM2G153488	5:187013898-187014947	85.941	197.26	0.017163	3.315671	Defensin and Defensin-like DEFL family
GRMZM2G030408	1:149968358-149978577	28.469	66.208	0.042767	3.379068	Predicted membrane protein
GRMZM2G028379	1:261468410-261472350	36.655	86.914	0.042767	3.474915	Related to Coiled-Coil-Helix Domain Containing 2 / NUR77
GRMZM2G077718	2:186257700-186258592	37.433	95.382	0.017163	3.855035	Unknown
H4C14	10:134829897-134830543	93.641	245.03	0.042767	4.005747	Histone H4C14
GRMZM2G156861	3:168738872-168882335	7.7186	21.078	0.017163	4.260259	LOX1 - Lipoxygenase1
GRMZM2G146206	8:168296434-168300637	6.3528	20.353	0.036917	5.364161	Ttriosephosphate isomerase
GRMZM2G019686	3:155132783-155133636	22.206	73.724	0.017163	5.647201	FPF1 flowering promoting factor 1
GRMZM2G326111	5:167791847-167793057	105.24	353.91	0.017163	5.752474	PPI1 - Peptidyl-prolyl isomerase1
GRMZM2G172491	4:3051214-3054036	13.018	47.179	0.017163	6.408659	BX4 - benzoxazinone synthesis4
GRMZM5G838907	2:11307185-11308450	18.122	69.303	0.017163	6.925498	Unknown, overlaps Mir169c
GRMZM2G146677	5:146880877-146886034	11.854	46.681	0.017163	7.224225	GOT3 - glutamate-oxaloacetic transaminase3
GRMZM2G057258	6:7149468-7151851	5.4926	32.189	0.017163	12.81966	Haloperoxidase-related
GRMZM2G101958	10:4168396-4169548	10.912	100.24	0.017163	24.51782	PLT1 - Phospholipid transfer protein homolog 1
GRMZM2G033544	4:1987655-1991701	1.741	19.424	0.017163	32.45485	Possible Cyclopropane-fatty-acyl-phospholipid synthase
GRMZM2G050875	6:105319100-105325570	9.8097	125.43	0.017163	39.50787	Related to EARLY RESPONSIVE TO DEHYDRATION 15
GRMZM2G034152	10:62260919-62265303	5.2592	70.909	0.017163	42.65054	PAO1 - Polyamine oxidase 1
GRMZM2G016890	10:34240658-34246077	33.471	573.48	0.017163	60.26611	GLU1 - beta glucosidase 1
GRMZM2G375733	4:68038684-68039894	0	8.5916	0.017163		Unknown
GRMZM2G171644	4:186770423-186771551	0	7.9699	0.017163		Unknown
GRMZM2G116881	6:107551094-107552151	0	6.8074	0.017163		Unknown Expressed Protein

Table2 – Differentially Expressed Genes: This spreadsheet is the output of the cuffdiff results. Gene identifier and position are given, along with the FPKM in

each triplicate sample. The q-value indicates the false-discovery rate corrected p-value for the test statistic. q-values below 0.05 were selected for this analysis. Finally, the fold change for the locus is given, along with a brief description.

Chapter 3 – Investigating Organogenic Processes in *Hoja loca*

Introduction

The *Hoja loca* defects in leaf initiation and leaf morphology show that basic shoot patterning occurs normally while dramatically affecting the initiation of lateral organs. In this chapter, I develop and use a variety of techniques to investigate how these processes are affected in *Hoja loca*.

PIN1 is known to play a crucial role in the development of the maize shoot (Forestan and Varotto 2012). Because of the defects in organ initiation and formation in *Hoja loca*, I sought to investigate the effect of the mutation on PIN1 expression and to look for genetic interactions. To do this, I developed antibodies against the four PIN1 homologs in maize and ordered transposon insertion knockout lines. Studying this protein family in maize has utility since the PIN1 family has expanded and subfunctionalized in the grasses (O'Connor et al. 2014). Brassica species including Arabidopsis lack one of the crucial PIN1 genes, sister-of-PIN (SoPIN). Characterizing the function of the PIN genes will aid our understanding of PIN-mediated auxin patterning outside of the Brassicas.

Further investigation of Hoja loca focuses on the expression of the *KNOTTED1* gene that promotes meristem identity (Kerstetter et al. 1997). Downregulation of *KNOTTED1* expression predicts the site of organ initiation and is required for organ formation (Jackson, Veit, and Hake 1994). Looking at the expression of *KNOTTED1* in *Hoja loca* will determine whether the disruption in organogenesis takes place before or after downregulation.

Finally, because of the possible involvement of flavonol in mediating the *Hoja loca* defect, its distribution throughout the maize shoot is analyzed.

Results

PIN knockout lines

Two approaches were used to obtain knockouts for the 4 PIN1 homologs in maize. Transposon insertions were obtained for PIN1a and PIN1b from the uniform mu stocks (McCarty et al. 2013). The PIN1a insertion was located in the 3' UTR, and the PIN1b insertion was near the end of the second exon. A Ds insertion was also obtained for PIN1a in the 5' UTR near the transcription start site. These insertions were introgressed into the A632 inbred and observed relative to their normal siblings. No morphological defects were observed. The pin1b mutant has been confirmed as an RNA knockout by RT-PCR (Figure 2A).

To account for possible gene redundancy, double *pin1a-Ds* and *pin1b-Mu* mutants were generated. Double homozygotes were identified, but phenotypic defects were not observed. Analysis was greatly complicated by the presence of other mutations in the genetic background as the material was insufficiently backcrossed.

The Trait Utility System for Corn (TUSC) was used to generate insertions in PIN1c and SoPIN. Several insertions into exons were verified, but poor germination and overall low plant vigor prevented these lines from being propagated. The mutant plants that did grow did not display any hallmark *pin* phenotypes, though had diminished spikelet formation (data not shown). However, without sufficient introgression into a well-characterized inbred, it is impossible to say whether this was caused by the insertion.

Antibody Production

Antibodies for the maize PIN1 homologs were generated against the hydrophilic intracellular loop of the proteins, as has been done with other PIN antibodies (Gälweiler et al. 1998). These sequences were cloned and inserted into vectors with 6His and GST tagging sequences. The 6His-tagged protein was used as antigen to inject into two guinea pigs for each protein (Figure 1A). The GST-tagged version was bound to columns to use for affinity purification (Figure 1B). The use of the small 6His epitope and a different tag for making affinity columns ensures high specificity to the desired antigen. Affinity purification was not performed on the PIN1c serum as the GST-tagged protein would not express.

Antibody specificity was assessed by Western Blot against the recombinant protein (Figure 1C). Against the GST-tagged protein, only anti-SoPIN displayed high specificity, even after very long exposure. Anti-PIN1a and anti-PIN1b both detected each other, while anti-PIN1c detected all 4 recombinant proteins. This is consistent with SoPIN being the most diverged from the other PINs (O'Connor et al. 2014). Against the 6His-tagged proteins, anti-PIN1a continued to show significant affinity for PIN1b, even greater than for the intended target PIN1a (Figure 1D). Anti-PIN1b, however, shows affinity only for the PIN1b protein, indicating it may be specific.

Immunolocalization with the PIN antibodies shows expression patterns consistent with those previously described for other PIN1 homologs (O'Connor et al. 2014; Carraro et al. 2006; Byeong-ha Lee et al. 2009). PIN1c was excluded from this analysis due to the inability to affinity purify the antibody and the low specificity the serum displays by Western Blot. The SoPIN antibody has the most distinct expression pattern, while PIN1a and PIN1b are quite similar. Some specificity between PIN1a and PIN1b can be observed, particularly in the root (Figures 2B and C). PIN1a can be seen polarized toward the root apex in the cortex tissues, while PIN1b is present more in the stele. However, using the pin1b knockout, anti-PIN1b signal is still detected (Figure 2E). This expression pattern is identical

to PIN1a, suggesting that the antibody has affinity for the PIN1a protein in immunolocalization (Figure 2D).

Anti-PIN1a Immunolocalization

Immunolocalization with the PIN1a antibody reveals and expression pattern consistent with previously reported results from a PIN:YFP reporter line (Lee et al., 2009). Expression mostly occurs along vascular traces in the SAM and inflorescence meristems (Figures 3A and B). Epidermal expression is seen at the sites of incipient organ formation, from new leaves to new floral organs in spikelet meristems (Figure 3C). Expression is seen to be polarized along the direction of auxin flow from organ initials, along vasculature, and down toward the root.

In the SAM, PIN1a appears to be excluded from the L1 and L2 layers, but is otherwise present internally (Figure 3A). At the P0, some polarization toward the local auxin maximum appears to be present (Figure 3D). This observation is not conclusive, however, as sectioned tissue can capture only parts of the plasma membrane, giving a two-dimensional view of a three-dimensional structure. This is not seen at the at the P1, were strong polar localization points internally (Figure 3E).

Hoja loca SAMs that are undergoing organ initiation failure do not have epidermal expression of PIN1a (Figure 3F). This sample is a SAM without a leaf at the expected site of the P1 leaf, as perhaps also the P2. There is also no PIN patterning indicating a P0. The internal expression also appears to be more disorganized with little clear polar PIN localization.

Anti-PIN1b Immunolocalization

The patterning of PIN1b is quite similar to PIN1a (Figures 4A and B). The primary difference between them is that the PIN1b antibody displays stronger polarization. It is difficult to say whether this is an actual difference in protein localization, or simply a consequence of the antibody providing less background signal. Spikelet PIN1b localization is also similar to PIN1a, reiterating the pattern of linking local auxin maxima with vascular sinks (Figure 4C).

PIN1b localization in *Hoja loca* again matches the PIN1a pattern. Clear vascular traces are seen connecting organs that succeed in forming, even if those organs have morphological defects. There is no signal found along any of the bare stem where leaf initiation has failed.

Anti-SoPIN Immunolocalization

The SoPIN expression pattern is quite distinct from the other PINs. Clear signal can be seen along the epidermis of the meristem flanks (Figure 5A). Polarized expression along the epidermis points toward developing organs. There is also expression in the internal tissues that is also polarized toward incipient and

developing organs. However, expression along mature vasculature is basal, with the direction of auxin flux.

The pattern continues in the IM (Figure 5B). Expression in the L1 layer is seen throughout the developing tassel, including along branches. Stronger signal is seen at developing spikelet pair meristems, where expression is not restricted to just the L1 layer (Figure 5B inset).

Expression in *Hoja loca* again shows that regions of bare stem where leaf initiation has failed do not expression patterns consistent with local auxin maxima (Figure 5C). The bare segments have expression in the epidermal layer, but polarization is directed toward the nearest organ. There is also no expression outside of the epidermal layer in these regions, whereas there is at the sites of successful organ initiation.

PIN1a:YFP Expression

The PIN1a:YFP reporter line provides a way to image whole tissue [Lee et al., 2009]. This was crossed with Hoja loca to observe the expression in mutant meristems where leaf initiation has failed. Expression along the vasculature and internal SAM tissues was normal, but distinct rings of PIN1a expression were observed along bare segments of stem (Figure 6 A-D). The numbers and spacing of these rings is consistent with the position of leaf primordia; the rings start at the meristem periphery and continue down until the next leaf. These rings are completely separate from the internal column of PIN1a expression (Figures 6A and C). These rings also completely encircle the stem, forming continuous discrete rings in many cases (Figure 6B). In cases where many initiation events have failed, the rings become less organized and intersect (Figure 6D).

DPBA Staining

Diphenylboric Acid 2-aminoethyl Ester is a florescent stain for flavonols in plants. Upon interaction with Kaempferol or Quercetin, it will floresce around 515nm and 530nm respectively (Lewis et al. 2011). This stain has been used to investigate the role of flavonols in auxin transport in the roots of Arabidopsis, but analysis of the shoot is lacking. Considering the possible effect ZmGLU1 has on flavonol accumulation, I sought to characterize flavonols in the maize shoot.
DPBA staining reveals extensive flavonol presence in the shoot, with very little background signal (Figure 7A and B). In the SAM, flavonol signal is primarily in the epidermal cells, particularly at the apex of the shoot. Signal can be seen in both the cytoplasm and in nuclei, consistent with previous reports and the localization of flavonol biosynthetic enzymes (Lewis et al. 2011; Saslowsky, Warek, and Winkel 2005).

DPBA staining is especially high at the sinus between leaf margins and surrounding the incipient leaf primordium (Figure 7C). This shows that flavonols

are present near the site of lateral organ initiation, as well as at distinct morphological zones of the leaf.

DPBA staining of a PIN1a:YFP reporter line shows that the domains of PIN1a expression and flavonols are mutually exclusive; flavonols are present between the devloping vasculature of young leaves, but excluded along the vascular traces and the leaf tip (Figure 7A-C). High flavonol signal also localized laterally in a band across the leaf. This is approximately the location of the pre-ligular band, though may be somewhat distal to it. At the leaf tip, high PIN1a:YFP signaling is seen, around which flavonols accumulate. This pattern is consistent across the observed tissues; flavonols appear to accumulate near zones of high auxin concentration, but are excluded from the maxima.

Attempts were made to image *Hoja loca* shoot apexes with DPBA, but useful images were difficult to collect. SAMs with no visible defects were indistinguishable from normal siblings (data not shown). The intensity of forescence was identical, and matched the diffuse signal throughout the apex. Specimens with visible defects had no staining along bare regions of stem, and the staining process resulted in what appeared to be tissue damage. Time restrictions prevented further analysis, though simple modifications to the protocol will likely yield good results.

KNOTTED1 Expression in *Hoja loca*

KNOTTED1 is normally present in meristem tissue, but downregulated in differentiated tissue (Jackson, Veit, and Hake 1994). In *Hoja loca*, this pattern remains with no signal in the leaves and strong signal throughout the meristem (Figure 8). The bare segment of stem where leaf initiation has failed shows strong KN1 accumulation, indicating that failure to initiate a leaf is also failure to downregulate KN1 (Figure 8 inset).

Discussion

Some progress was made in developing PIN knockout lines, but only PIN1b could be verified as an RNA-knockdown. The insertions into PIN1a were not located in coding sequence, and reliable genotyping was difficult to develop. Given the similarities between PIN1a, b, and c, it is not surprising that a single knockout would display no mutant phenotype. Without a SoPIN mutant, the usefulness of this project seemed limited and further attempts to develop a *pin1a* and *pin1b* double mutant were not pursued.

The antibody project fared much better, resulting in 3 purified antibodies effective in a variety of assays. The distinctive localization pattern of SoPIN suggests it is highly specific, and it matches the localization found in *Brachypodium* (O'Connor et al. 2014). This tool is valuable for investigating SoPIN in a variety of mutants and species. The PIN1a and PIN1b antibodies match the general pattern of PIN1 expression seen in *Brachypodium* and *Zea mays* (Byeong-ha Lee et al. 2009). There are differences between their localization patterns in

immunolocalization, but specificity is not seen by Western Blot. Some anti-PIN1b signal can also be seen in *pin1b* knockouts. Further specificity could be acquired by purifying remaining serum against a smaller protein epitope that is divergent.

The immunolocalization patterns confirm the findings of O'Connor et al., 2014 that SoPIN is expressed primarily in epidermal cells and polarized toward auxin maxima, while PIN1a and PIN1b trace vasculature and are polarized away from sites of organ initiation. In *Hoja loca*, this pattern remains and no signs of PIN expression consistent with the formation of an auxin maximum are found along bare sections of stem.

In contrast to the results from immunolocalization, the PIN1a:YFP reporter line shows conspicuous rings of PIN1a expression along the meristem flanks. These results are not necessarily contradictory; thin sections used in immunolocalization can make it difficult to detect signal on the surface of tissue, and the material analyzed is different. The PIN1a:YPF rings are seen in older tissue, whereas the immunolocalization is best performed with younger tissue.

The ring shape of PIN1a expression is very interesting. *pin1* mutants in Arabidopsis make a similar ring of *LFY* and *ANT* expression encircling the inflorescence apex (Vernoux et al. 2000). The authors of that paper interpret link this observation with organogenesis failure: "This could imply that the mutant simply forms one ring like 'anlage' which then fails to grow out." A similar process could be acting in *Hoja loca*, with the notable difference that it makes many successive rings, and can recover to form more leaves in later initiation events. It is also interesting that *Hoja loca* leaf morphology is defective in medial-lateral patterning which matches this expression pattern. Instead of forming discrete primordia that mark the medial domain, these encircling primordia lack medial-lateral asymmetry.

While rings in PIN expression form along bare sections of stem, *KNOTTED1* remains expressed along these regions. This suggests that, while PIN1a may be recruited in rings at sites of failed leaf initiation, the process of organogenesis fails before *KN1* downregulation. Furthermore, *KN1* downregulation must not be required for defining phytomer nodes, since mutant plants always display proper internode elongation.

Finally, DPBA staining reveals that flavonols are present in the shoot, and are localized in patterns related to auxin patterns. Auxin and flavonol form mutually exclusive domains in young leaves, suggesting that auxin signaling could influence flavonol levels. Flavonols are also found adjacent to the site of organ initiation, but excluded from the presumptive site of initiation itself. These observations suggest that flavonol patterning could be involved in developmental patterning. An attractive hypothesis is that, since flavonols are thought to restrict auxin flow, they could accumulate in tissues adjacent to high auxin levels to reinforce auxin patterning.

Figures

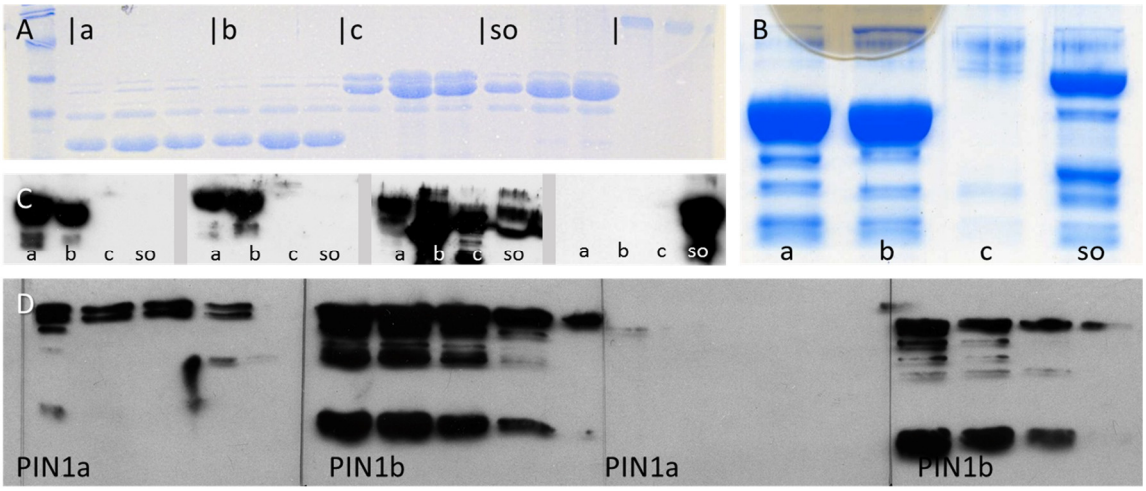

Figure 1: Recombinant PIN Proteins and Western Blots. (A) Coomassie stained PAGE of 6-His-tagged proteins. (B) Coomassie stained PAGE of GST-tagged PIN proteins. (C) Western Blot of purified antibody (a, b, and So) and serum (c) against GST-tagged recombinant protein. (D) Western Blot of 6-His-tagged PIN1a and PIN1b protein with anti-PIN1a (left half of blot) and anti-PIN1b (right half of gel). Protein loading decreases moving left.

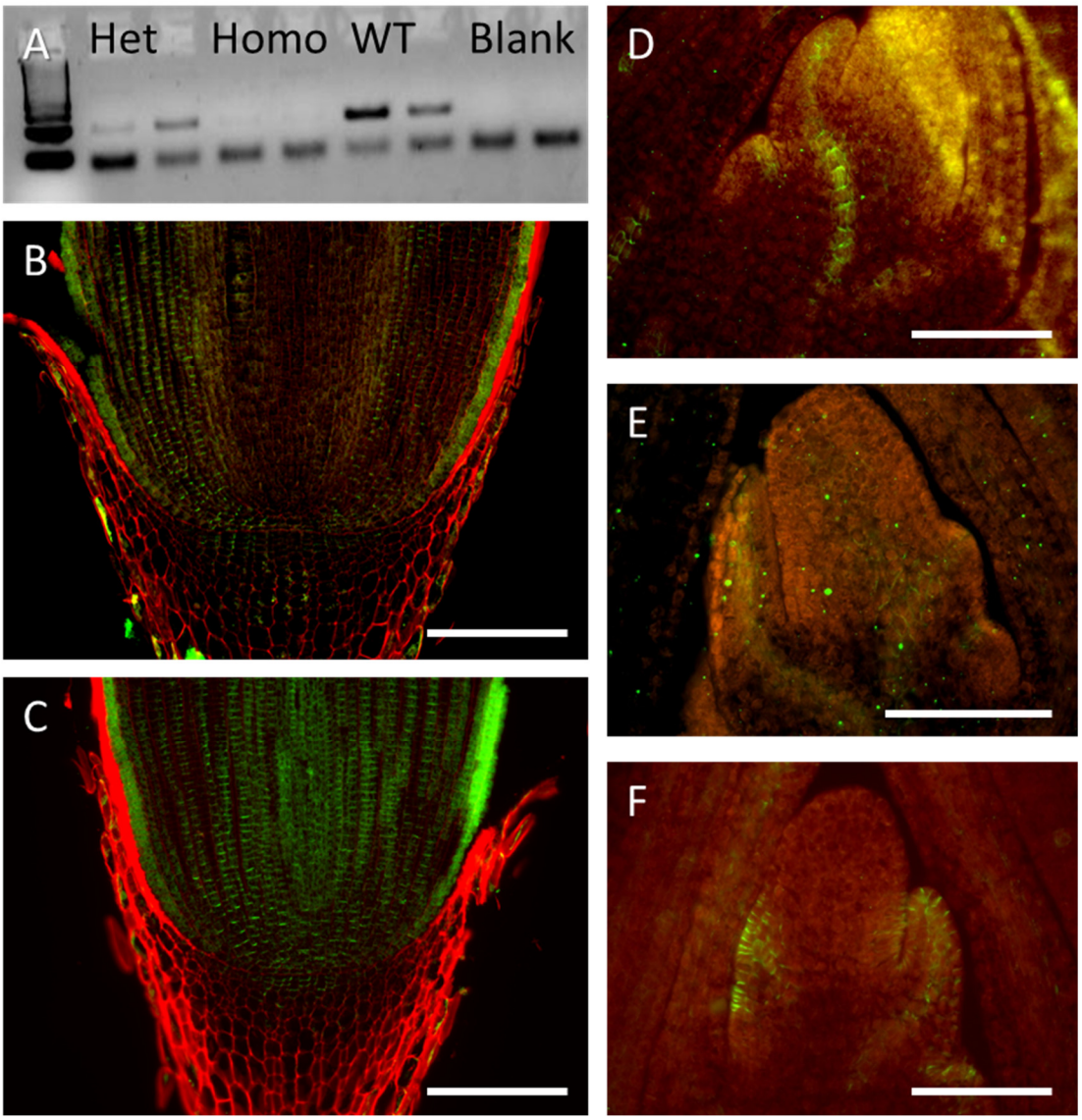

Figure 2: *pin1b* Mutant. (A) RT-PCR amplicons for Pin1b imaged on RNA gel. Two samples each of heterozygous *pin1b* mutants, homozygotes, normal siblings, and no-DNA blank. (B) anti-PIN1a immunolocalization in root apex showing signal predominantly in the cortex. Scale = 300um (C) anti-PIN1b immunolocalization in the root apex showing signal throughout the root, though excluded from the root cap. (D) anti-PIN1a in the *pin1b* mutant. Scale = 150um (E) anti-PIN1b in the *pin1b* mutant. (F) anti-SoPIN in the *pin1b* mutant.

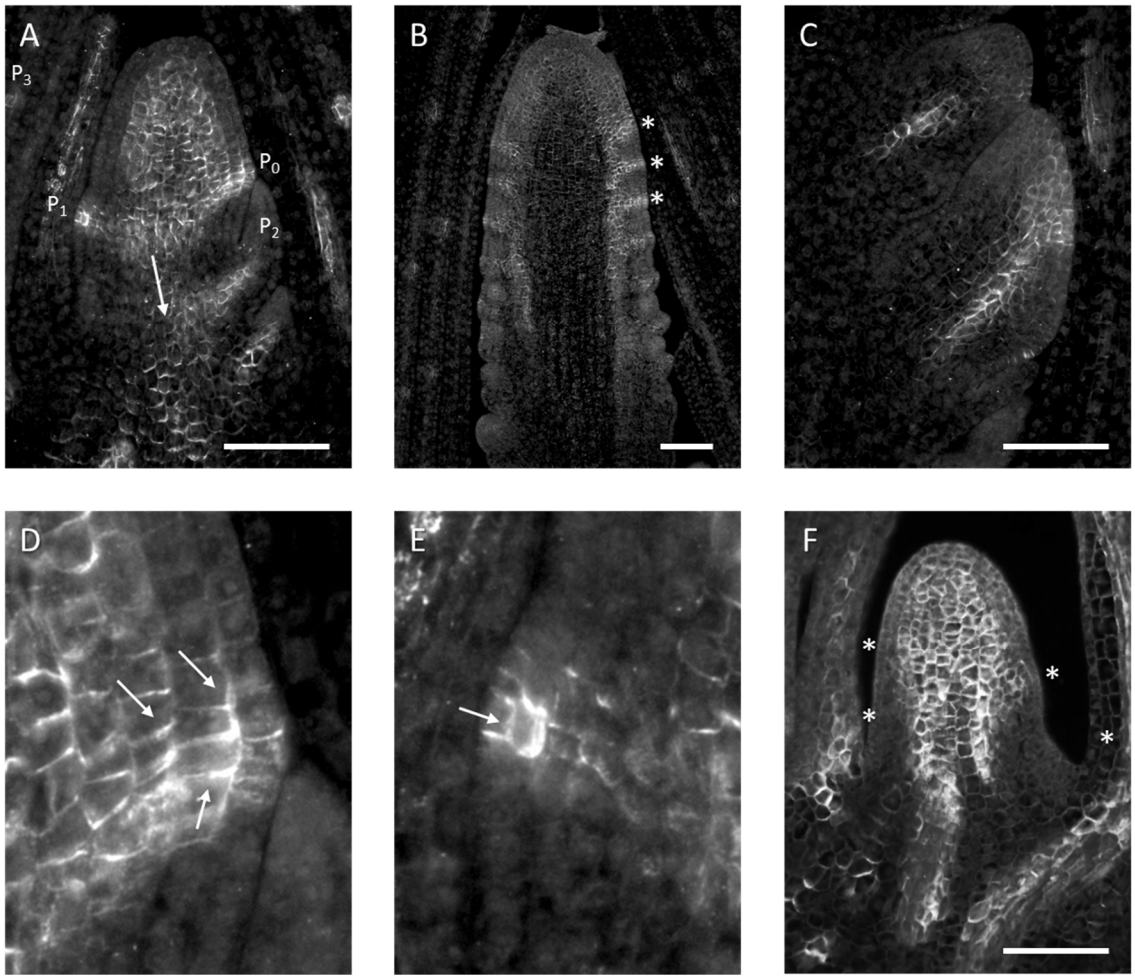

Figure 3: PIN1a Immunolocalization. (A) anti-PIN1a signal in the maize shoot apex. Signal is seen strongly marking lateral organ primordia and developing vasculature. The direction of PIN1a localization is basal along the vasculature. Scale = 150um (B) anti-PIN1a signal in the maize inflorescence. Spikelet pair meristem primordia are visible (stars). Scale = 300um (C) Signal in developing spikelets. Scale = 150um (D) Closeup of P0 primordia from part A showing polarization toward the auxin maximum (arrows). (D) Closeup of P1 showing polarization directing internally toward the developing vasculature (arrow). (F) anti-PIN1a signal in an *Hoja loca* shoot apex. This specimen as no sign of PIN1a signal at the presumed sites of lateral organ initation in P_0, P_1, and P_2. Overall PIN1a expression is more diffuse, perhaps due to no vasculature forming in the absence of lateral organs. Scale = 150um

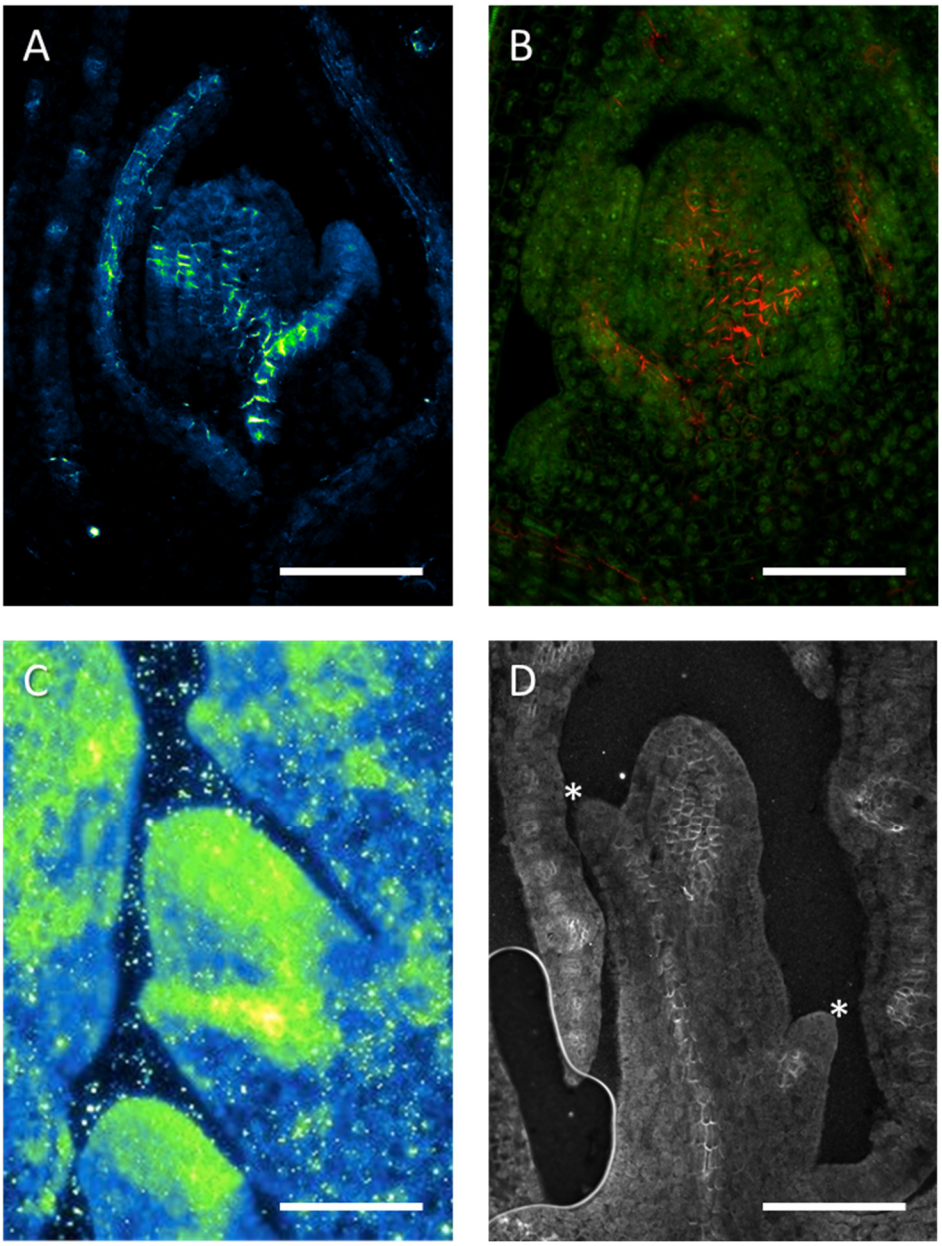

Figure 4: PIN1b Immunolocalization. (A) anti-PIN1b signal in a maize shoot apex. Signal is seen along developing vasculature and is strongly polarized (arrow). Scale = 150um (B) Another view of PIN1b, again showing strongly polarized localization. Scale = 150um (C) anti-PIN1b signal in a young spikelet. Scale = 75um (D) anti-PIN1b signal in an *Hoja loca* shoot apex that has formed partial lateral organs (stars). PIN1b can be seen only where lateral organs have formed, and along vasculature. No expression is seen along bare sections of stem. Scale = 300um

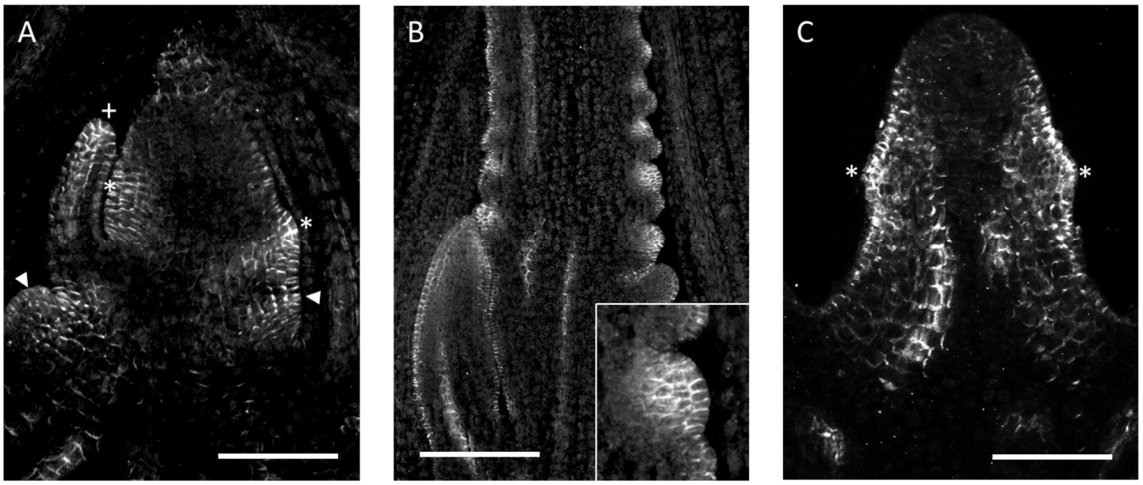

Figure 5: SoPIN Immunolocalization. (A) anti-SoPIN signal in a shoot apex. Strongest signal is seen at sites of lateral organ initiation (stars), at leaf tips (cross), and at the leaf axil (arrows). Polar localization is directed toward organ tips and presumptive auxin maxima. Scale = 150um (B) anti-SoPIN signal in a developing tassel. Strongest expression is seen at the tips of lateral organs, with polarization directed toward the tips (inset). Scale = 300um (C) anti-SoPIN signal in an *Hoja loca* shoot apex. Expression is seen at an encircling leaf primordium, with little signal along the bare sections of stem. Polarization is directed toward this organ only (stars). Scale = 150um

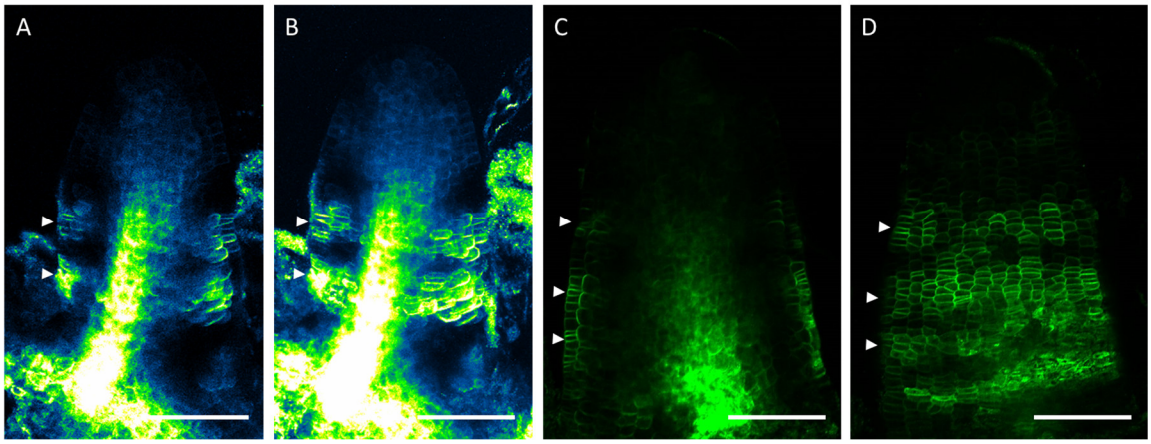

Figure 6: PIN1a:YFP in *Hoja loca*. (A) PIN1a:YFP signal in a young maize shoot. Two distinct rings of PIN1a expression are seen encircling the SAM (arrows). There is also a large central column of PIN1a expression. This medial optical section shows that the rings and central column do not connect. (B) Another view of the same shoot apex with an optical section closer to the front surface of the SAM. (C and D) PIN1a:YFP expression in an older *Hoja loca* shoot. Distinct rings of PIN1a expression are seen encircling the shoot (arrows). These rings are also disconnected from the central column of central PIN1a expression. Cells just below the epidermal layer have clearly polarized PIN1a expression toward the epidermal cells, suggesting auxin transport toward the surface. Scale = 150um in all panels.

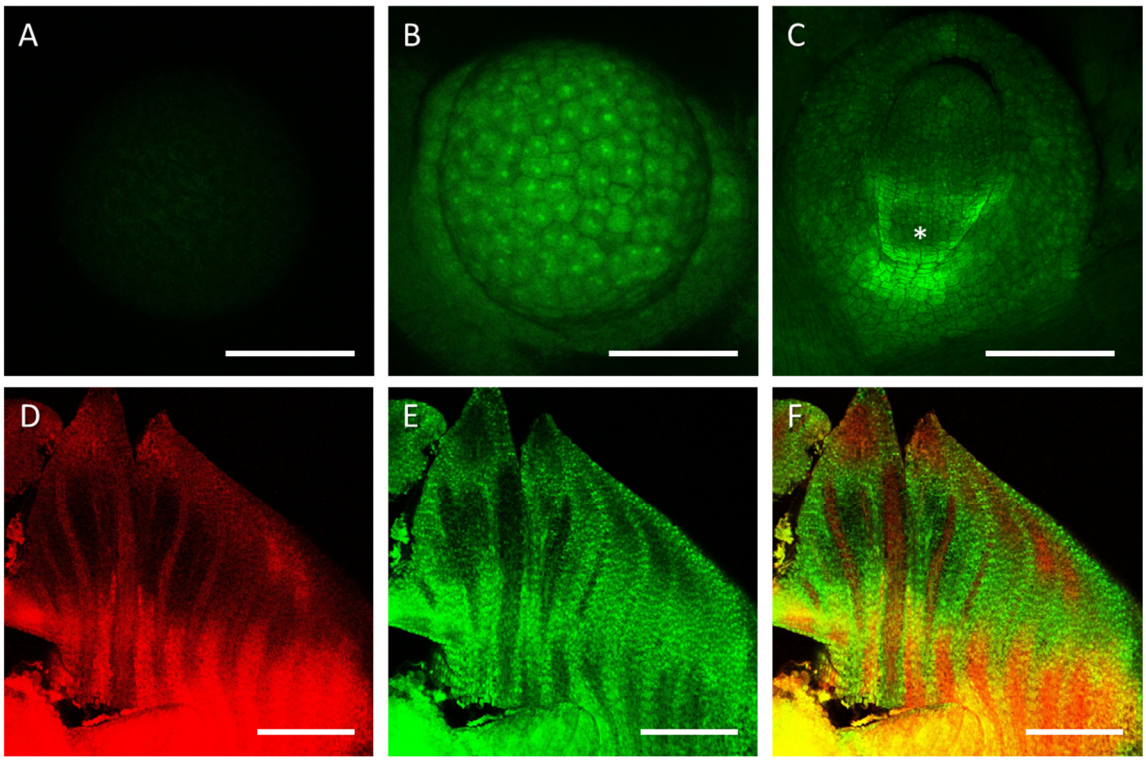

Figure 7: Flavonols in the Maize Shoot. (A) Background florescence in an unstained SAM. (B) DPBA signal in a maize SAM. Signal is seen throughout cells, with higher concentrations in nuclei. Signal is higher in the SAM than in the young leaves, and some increased signal is seen at leaf tips. (C) A side view of the SAM showing signal around the P_0 (star) and at the sinus between the leaf margins of P_2. (D) PIN1a:YPF signal in a young maize leaf. Expression is seen along the vasculature and leaf tip. (E) DPBA signal in the same leaf. (F) Combination of C and D showing that these signals occupy mutually exclusive domains in the leaf. Scale = 100um in all panels

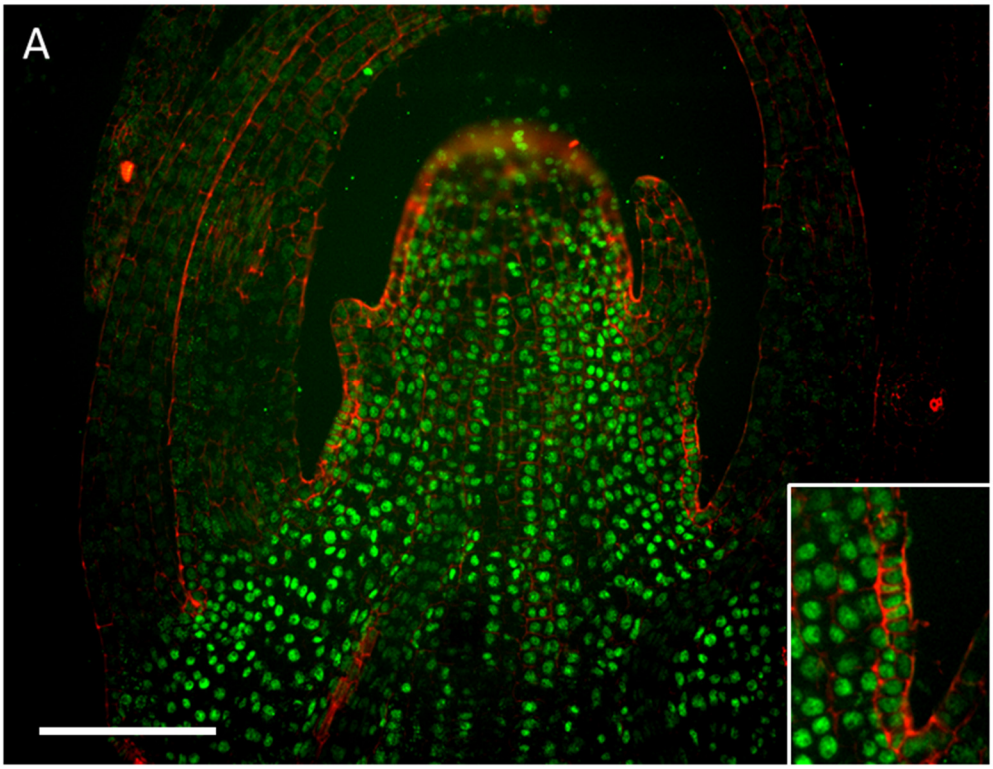

Figure 8: KNOTTED1 in *Hoja loca*. (A) anti-KN1 signal in a *Hoja loca* shoot apex. No signal is seen in leaves, yet clear signal is seen in the nuclei of cells along the bare section of stem where leaf initiation has not occurred (inset). Scale = 200um

Methods

Antibody Generation: Antibodies were produced as described in Chuck et al., 2010. The cytosolic loop of the *Pin* genes was cloned into pENTER, and then recombined into destination vectors with the HIS and GST tags. Recombinant HIS-tagged protein was injected into two Guinea Pigs for each gene. Affinity purification was performed with columns made with the GST-tagged recombinant protein.

Immunolocalization: Immunolocalization was performed as described in Lee et al., 2009. Primary antibody dilution was 1:200 in PBS for all antibodies, including secondary Cy3-conjugated anti-guinea pig (Jackson ImmunoResearch Laboratory). Samples were imaged on Axiovert (Zeiss).

PIN Insertions: Transposon insertions for *Pin1a* and *Pin1b* were obtained from MaizeGDB (http://www.maizegdb.org/data_center/stock) from the UniformMu population [Settles et al., 2007]. Transposon insertions for *Pin1c* and *SoPin* were obtained from R. Meeley via Trait Utility System for Corn (TUSC) (Pioneer Hi-Bred International)

Protein Blot Analysis: 8% SDS-polyacrylamide gels were run at 200V for 30-60 minutes and blotted onto a polyvinylidene fluoride membrane (Millipore) using a transfer cell (Bio-Rad). Blocking performed in 5% nonfat milk in TBS-T buffer (140 mM NaCl, 20 mM Tris, pH 7.6, and 0.1% [v/v] Tween 20) for 1 h. Antibody diluted 1:1,000 was incubated with the blocked membrane for 1 h. After washing three times with TBS-T for 10 min, a horseradish peroxidase labeled anti-guinea pig antibody (Amersham Bioscience) was used at 1:5,000 for secondary antibody labeling. Membranes were washed 4 times and visualized with the ECL Plus Western Blotting Detection System (Amersham Bioscience) and then exposed to x-ray film from 1 to 10 minutes.

Conclusions and Future Directions

Hoja loca is an exciting developmental mutation that should provide insight into the process of lateral organ organogenesis. The mutant effect is specific to lateral organ initiation, avoiding complications from changes to shoot architecture or meristem maintenance. Robust internode formation shows that, even when leaves are not formed, mutants are still organized into phytomer units, demonstrating that lateral organ formation is not required to create distinct plant nodes. The mutant defects in leaf development show that the formation of distinct medial and lateral domains are important for proper organ initiation. Patterning along the proximal-distal and abaxial-adaxial axes are unaffected in *Hoja loca*, while the formation of the medial midrib and separation of the lateral margins is aberrant.

Another maize mutant shares some aspects of the Hoja loca phenotype: *barren inflorescence 2* (*bif2*) (McSteen et al. 2007). *bif2* plants also form leaves lacking a midrib, and organ initiation is defective in the inflorescence, relating these phenotypes once again. BIF2 is a co-ortholog of PINOID, a serine/threonine kinase that is involved in PIN polarization and auxin patterning. The identification of Hoja loca as ZmIAA38 shows that auxin mediates the mutant phenotypes of both mutants. PIN1a expression is altered in both mutants such that concentrated local auxin maxima cannot form on the meristem periphery. BIF2 directly phosphylates PIN1a, likely directly affecting its localization. ZmIAA38 could be involved in feedback cycles that promote local auxin maxima.

While the mechanism of disrupting auxin patterning in *Hoja loca* is unknown, the highly upregulated gene ZmGLU1 provides some compelling hints. Glucosidases like ZmGLU1 are known to degrade flavonols and activate cytokinin-glucoside conjugates. Flavonols are known to affect auxin transport, and cytokinin signaling is often closely related to auxin signaling, generally in an antagonistic manner. Investigating the activity of ZmGLU1 will be crucial for understanding *Hoja loca*. This gene is also implicated in ligule development, making it a keystone for understanding other aspects of maize organogenesis.

Several experiments will could provide valuable insight into the *Hoja loca* defect and organogenesis. Generating knockout mutants for ZmIAA38 and ZmGLU1

are natural next steps in understanding the genetic interactions and functions of these genes. It is particularly interesting that upregulation of ZmGLU1 occurs at ligule formation, but the ectopic levels in *Hoja loca* result in failed organ initiation. The possibility that defined levels (not too much nor too little) of ZmGLU1 expression are needed for organogenesis is consistent with the phenocritical nature of the *Hoja loca* defect.

It will also be important to characterize flavonols and cytokinin signaling in *Hoja loca*. Both compounds could conceivably mediate the effects on auxin patterning and organogenesis. Given that flavonols accumulate around the site of leaf initiation, ZmGLU1 may be responsible for excluding them from the auxin maximum, or perhaps favor certain flavonol-glucoside conjugates with different activities. Or, auxin-dependent downregulation of ZmGLU1 via ZmIAA38 could be required to limit Cytokinin signaling at the site of organogenesis. Ectopic ZmGLU1 expression in *Hoja loca* could lead to cytokinin signaling that interferes with organogenesis.

While much remains unknown, *Hoja loca* presents compelling opportunities to investigate organogenesis in plants.

References

Abel, S, P W Oeller, and A Theologis. 1994. “Early Auxin-Induced Genes Encode Short-Lived Nuclear Proteins.” *Proceedings of the National Academy of Sciences of the United States of America* 91 (1): 326–30.

Adamowski, Maciek, and Jiří Friml. 2015. “PIN-Dependent Auxin Transport: Action, Regulation, and Evolution.” *The Plant Cell* 27 (1): 20–32. doi:10.1105/tpc.114.134874.

Alkio, Merianne, Tomoko M. Tabuchi, Xuchen Wang, and Adán Colón-Carmona. 2005. “Stress Responses to Polycyclic Aromatic Hydrocarbons in Arabidopsis Include Growth Inhibition and Hypersensitive Response-like Symptoms.” *Journal of Experimental Botany* 56 (421): 2983–94. doi:10.1093/jxb/eri295.

Bayer, E M, R S Smith, T Mandel, N Nakayama, M Sauer, P Prusinkiewicz, and C Kuhlemeier. 2009. “Integration of Transport-Based Models for Phyllotaxis and Midvein Formation.” *Genes & Development* 23 (3): 373–84.

Benjamins, René, Ab Quint, Dolf Weijers, Paul Hooykaas, and Remko Offringa. 2001. “The PINOID Protein Kinase Regulates Organ Development in Arabidopsis by Enhancing Polar Auxin Transport.” *Development* 128 (20): 4057–67.

Benková, Eva, Marta Michniewicz, Michael Sauer, Thomas Teichmann, Daniela Seifertová, Gerd Jürgens, and Jirí Friml. 2003. “Local, Efflux-Dependent Auxin Gradients as a Common Module for Plant Organ Formation.” *Cell* 115 (5): 591–602.

Besnard, Fabrice, Yassin Refahi, Valérie Morin, Benjamin Marteaux, Géraldine Brunoud, Pierre Chambrier, Frédérique Rozier, et al. 2014. “Cytokinin Signalling Inhibitory Fields Provide Robustness to Phyllotaxis.” *Nature* 505

(7483): 417–21. doi:10.1038/nature12791.
Boer, D Roeland, Alejandra Freire-Rios, Willy A M van den Berg, Terrens Saaki, Iain W Manfield, Stefan Kepinski, Irene López-Vidrieo, et al. 2014. “Structural Basis for DNA Binding Specificity by the Auxin-Dependent ARF Transcription Factors.” *Cell* 156 (3): 577–89. doi:10.1016/j.cell.2013.12.027.
Bortiri, Esteban, Dave Jackson, and Sarah Hake. 2006. “Advances in Maize Genomics: The Emergence of Positional Cloning.” *Current Opinion in Plant Biology* 9 (2). Plant Gene Expression Center, USDA-ARS, and Plant and Microbial Biology Department, University of California, Berkeley, 800 Buchanan Avenue, Albany, California 94710, USA.: Elsevier Ltd: 164–71.
Brown, D E, A M Rashotte, A S Murphy, J Normanly, B W Tague, W A Peer, L Taiz, and G K Muday. 2001. “Flavonoids Act as Negative Regulators of Auxin Transport in Vivo in Arabidopsis.” *Plant Physiology* 126 (2): 524–35.
Brzobohatý, B, I Moore, P Kristoffersen, L Bako, N Campos, J Schell, and K Palme. 1993. “Release of Active Cytokinin by a Beta-Glucosidase Localized to the Maize Root Meristem.” *Science (New York, N.Y.)* 262 (5136): 1051–54.
Buer, Charles S, and Gloria K Muday. 2004. “The Transparent testa4 Mutation Prevents Flavonoid Synthesis and Alters Auxin Transport and the Response of Arabidopsis Roots to Gravity and Light.” *The Plant Cell* 16 (5): 1191–1205. doi:10.1105/tpc.020313.
Calderón Villalobos, Luz Irina A, Sarah Lee, Cesar De Oliveira, Anthony Ivetac, Wolfgang Brandt, Lynne Armitage, Laura B Sheard, et al. 2012. “A Combinatorial TIR1/AFB-Aux/IAA Co-Receptor System for Differential Sensing of Auxin.” *Nature Chemical Biology* 8 (5): 477–85. doi:10.1038/nchembio.926.
Campos, Narciso, Laszlo Bako, Joachim Feldwisch, Jeff Schell, and Klaus Palme. 1992. “A Protein from Maize Labeled with Azido-IAA Has Novel β-Glucosidase Activity.” *The Plant Journal* 2 (5): 675–84. doi:10.1111/j.1365-313X.1992.tb00136.x.
Carraro, Nicola, Cristian Forestan, Sabrina Canova, Jan Traas, and Serena Varotto. 2006. “ZmPIN1a and ZmPIN1b Encode Two Novel Putative Candidates for Polar Auxin Transport and Plant Architecture Determination of Maize.” *Plant Physiology* 142 (1): 254–64. doi:10.1104/pp.106.080119.
Cho, Hyunwoo, Hojin Ryu, Sangchul Rho, Kristine Hill, Stephanie Smith, Dominique Audenaert, Joonghyuk Park, et al. 2014. “A Secreted Peptide Acts on BIN2-Mediated Phosphorylation of ARFs to Potentiate Auxin Response during Lateral Root Development.” *Nature Cell Biology* 16 (1): 66–76. doi:10.1038/ncb2893.
Choi, G, H Yi, J Lee, Y K Kwon, M S Soh, B Shin, Z Luka, T R Hahn, and P S Song. 1999. “Phytochrome Signalling Is Mediated through Nucleoside Diphosphate Kinase 2.” *Nature* 401 (6753): 610–13. doi:10.1038/44176.
Collum, Tamara D, Meenu S Padmanabhan, Yi-Cheng Hsieh, and James N Culver. 2016. “Tobacco Mosaic Virus-Directed Reprogramming of Auxin/indole Acetic Acid Protein Transcriptional Responses Enhances Virus Phloem Loading.” *Proceedings of the National Academy of Sciences of the*

United States of America, April, 1524390113 – . doi:10.1073/pnas.1524390113.
Dharmasiri, Nihal, Sunethra Dharmasiri, and Mark Estelle. 2005. “The F-Box Protein TIR1 Is an Auxin Receptor.” *Nature* 435 (7041): 441–45. doi:10.1038/nature03543.
Eklöf, S, C Astot, F Sitbon, T Moritz, O Olsson, and G Sandberg. 2000. “Transgenic Tobacco Plants Co-Expressing Agrobacterium Iaa and Ipt Genes Have Wild-Type Hormone Levels but Display Both Auxin- and Cytokinin-Overproducing Phenotypes.” *The Plant Journal : For Cell and Molecular Biology* 23 (2): 279–84.
Eliasson, L, G Bertell, and E Bolander. 1989. “Inhibitory Action of Auxin on Root Elongation Not Mediated by Ethylene.” *Plant Physiology* 91 (1): 310–14.
Escamilla-Treviño, Luis L, Wei Chen, Marcella L Card, Ming-Che Shih, Chi-Lien Cheng, and Jonathan E Poulton. 2006. “Arabidopsis Thaliana Beta-Glucosidases BGLU45 and BGLU46 Hydrolyse Monolignol Glucosides.” *Phytochemistry* 67 (15): 1651–60. doi:10.1016/j.phytochem.2006.05.022.
Fiorillo, Annarita, Rodolfo Federico, Fabio Polticelli, Alberto Boffi, Franco Mazzei, Massimo Di Fusco, Andrea Ilari, and Paraskevi Tavladoraki. 2011. “The Structure of Maize Polyamine Oxidase K300M Mutant in Complex with the Natural Substrates Provides a Snapshot of the Catalytic Mechanism of Polyamine Oxidation.” *The FEBS Journal* 278 (5): 809–21. doi:10.1111/j.1742-4658.2010.08000.x.
Forestan, C, and S Varotto. 2012. “The Role of PIN Auxin Efflux Carriers in Polar Auxin Transport and Accumulation and Their Effect on Shaping Maize Development.” *Molecular Plant* 5 (4): 787–98.
Friml, Jirí, Anne Vieten, Michael Sauer, Dolf Weijers, Heinz Schwarz, Thorsten Hamann, Remko Offringa, and Gerd Jürgens. 2003. “Efflux-Dependent Auxin Gradients Establish the Apical-Basal Axis of Arabidopsis.” *Nature* 426 (6963): 147–53. doi:10.1038/nature02085.
Furutani, Masahiko, Yasukazu Nakano, and Masao Tasaka. 2014. “MAB4-Induced Auxin Sink Generates Local Auxin Gradients in Arabidopsis Organ Formation.” *Proceedings of the National Academy of Sciences of the United States of America* 111 (3): 1198–1203. doi:10.1073/pnas.1316109111.
Furutani, Masahiko, Norihito Sakamoto, Shuhei Yoshida, Takahito Kajiwara, Hélène S Robert, Jirí Friml, and Masao Tasaka. 2011. “Polar-Localized NPH3-like Proteins Regulate Polarity and Endocytosis of PIN-FORMED Auxin Efflux Carriers.” *Development (Cambridge, England)* 138 (10): 2069–78. doi:10.1242/dev.057745.
Galinat, Walton C. 1959. “THE PHYTOMER IN RELATION TO FLORAL HOMOLOGIES IN THE AMERICAN MAYDEAE.” *Harvard University Herbaria*. https://www.jstor.org/stable/41762203?seq=1#page_scan_tab_contents.
Gälweiler, L, C Guan, A Müller, E Wisman, K Mendgen, A Yephremov, and K Palme. 1998. “Regulation of Polar Auxin Transport by AtPIN1 in Arabidopsis Vascular Tissue.” *Science (New York, N.Y.)* 282 (5397): 2226–30.
Gao, Jian-Jie, Xue-Fang Shen, Ri-He Peng, Bo Zhu, Jing Xu, Hong-Juan Han,

and Quan-Hong Yao. 2012. “Phytoremediation and Phytosensing of Chemical Contaminant, Toluene: Identification of the Required Target Genes.” *Molecular Biology Reports* 39 (8): 8159–67. doi:10.1007/s11033-012-1663-3.

Geisler, Markus, and Angus S Murphy. 2006. “The ABC of Auxin Transport: The Role of P-Glycoproteins in Plant Development.” *FEBS Letters* 580 (4). Zurich-Basel Plant Science Center, Institute of Plant Biology, University of Zurich, CH-8007 Zurich, Switzerland. markus.geisler@botinst.unizh.ch: 1094–1102.

Gray, W M, S Kepinski, D Rouse, O Leyser, and M Estelle. 2001. “Auxin Regulates SCF(TIR1)-Dependent Degradation of AUX/IAA Proteins.” *Nature* 414 (6861): 271–76. doi:10.1038/35104500.

Griffiths, Anthony JF, Jeffrey H Miller, David T Suzuki, Richard C Lewontin, and William M Gelbart. 2000. “Induced Mutations.” W. H. Freeman.

Grunewald, Wim, Ive De Smet, Daniel R Lewis, Christian Löfke, Leentje Jansen, Geert Goeminne, Robin Vanden Bossche, et al. 2012. “Transcription Factor WRKY23 Assists Auxin Distribution Patterns during Arabidopsis Root Development through Local Control on Flavonol Biosynthesis.” *Proceedings of the National Academy of Sciences of the United States of America* 109 (5): 1554–59. doi:10.1073/pnas.1121134109.

Guenot, B., E. Bayer, D. Kierzkowski, R. S. Smith, T. Mandel, P. Zadnikova, E. Benkova, and C. Kuhlemeier. 2012. “PIN1-Independent Leaf Initiation in Arabidopsis.” *PLANT PHYSIOLOGY*. doi:10.1104/pp.112.200402.

Heisler, M G, C Ohno, P Das, P Sieber, G V Reddy, J A Long, and E M Meyerowitz. 2005. “Patterns of Auxin Transport and Gene Expression during Primordium Development Revealed by Live Imaging of the Arabidopsis Inflorescence Meristem.” *Current Biology : CB* 15 (21). Elsevier: 1899–1911.

Henrichs, Sina, Bangjun Wang, Yoichiro Fukao, Jinsheng Zhu, Laurence Charrier, Aurélien Bailly, Sophie C Oehring, et al. 2012. “Regulation of ABCB1/PGP1-Catalysed Auxin Transport by Linker Phosphorylation.” *The EMBO Journal* 31 (13). EMBO Press: 2965–80. doi:10.1038/emboj.2012.120.

Jackson, D., B. Veit, and S. Hake. 1994. “Expression of Maize KNOTTED1 Related Homeobox Genes in the Shoot Apical Meristem Predicts Patterns of Morphogenesis in the Vegetative Shoot.” *Development* 120 (2): 405–13.

Jacobs, M, and P H Rubery. 1988. “Naturally Occurring Auxin Transport Regulators.” *Science (New York, N.Y.)* 241 (4863): 346–49. doi:10.1126/science.241.4863.346.

Johnston, Robyn, Minghui Wang, Qi Sun, Anne W Sylvester, Sarah Hake, and Michael J Scanlon. 2014. “Transcriptomic Analyses Indicate That Maize Ligule Development Recapitulates Gene Expression Patterns That Occur during Lateral Organ Initiation.” *The Plant Cell*, 1–16. doi:10.1105/tpc.114.132688.

Kariola, Tarja, Günter Brader, Elina Helenius, Jing Li, Pekka Heino, and E Tapio Palva. 2006. “EARLY RESPONSIVE TO DEHYDRATION 15, a Negative Regulator of Abscisic Acid Responses in Arabidopsis.” *Plant Physiology* 142

(4): 1559–73. doi:10.1104/pp.106.086223.
Kepinski, Stefan, and Ottoline Leyser. 2005. “The Arabidopsis F-Box Protein TIR1 Is an Auxin Receptor.” *Nature* 435 (7041): 446–51. doi:10.1038/nature03542.
Kerstetter, R A, D Laudencia-Chingcuanco, L G Smith, and S Hake. 1997. “Loss-of-Function Mutations in the Maize Homeobox Gene, knotted1, Are Defective in Shoot Meristem Maintenance.” *Development* 124 (16). Plant and Microbial Biology Department, University of California, Berkeley 94720, USA.: 3045–54.
Kiran, Nagavalli S, Lenka Polanská, Radka Fohlerová, Pavel Mazura, Martina Válková, Miloslav Smeral, Jan Zouhar, et al. 2006. “Ectopic over-Expression of the Maize Beta-Glucosidase Zm-p60.1 Perturbs Cytokinin Homeostasis in Transgenic Tobacco.” *Journal of Experimental Botany* 57 (4): 985–96. doi:10.1093/jxb/erj084.
Korasick, David A, Corey S Westfall, Soon Goo Lee, Max H Nanao, Renaud Dumas, Gretchen Hagen, Thomas J Guilfoyle, Joseph M Jez, and Lucia C Strader. 2014. “Molecular Basis for AUXIN RESPONSE FACTOR Protein Interaction and the Control of Auxin Response Repression.” *Proceedings of the National Academy of Sciences of the United States of America* 111 (14): 5427–32. doi:10.1073/pnas.1400074111.
Kristoffersen, P, B Brzobohaty, I Höhfeld, L Bako, M Melkonian, and K Palme. 2000. “Developmental Regulation of the Maize Zm-p60.1 Gene Encoding a Beta-Glucosidase Located to Plastids.” *Planta* 210 (3): 407–15.
Kurakawa, Takashi, Nanae Ueda, Masahiko Maekawa, Kaoru Kobayashi, Mikiko Kojima, Yasuo Nagato, Hitoshi Sakakibara, and Junko Kyozuka. 2007. “Direct Control of Shoot Meristem Activity by a Cytokinin-Activating Enzyme.” *Nature* 445 (7128). Nature Publishing Group: 652–55.
Kuroha, Takeshi, Hiroki Tokunaga, Mikiko Kojima, Nanae Ueda, Takashi Ishida, Shingo Nagawa, Hiroo Fukuda, Keiko Sugimoto, and Hitoshi Sakakibara. 2009. “Functional Analyses of LONELY GUY Cytokinin-Activating Enzymes Reveal the Importance of the Direct Activation Pathway in Arabidopsis.” *The Plant Cell* 21 (10): 3152–69. doi:10.1105/tpc.109.068676.
Laluk, Kristin, Hongli Luo, Maofeng Chai, Rahul Dhawan, Zhibing Lai, and Tesfaye Mengiste. 2011. “Biochemical and Genetic Requirements for Function of the Immune Response Regulator BOTRYTIS-INDUCED KINASE1 in Plant Growth, Ethylene Signaling, and PAMP-Triggered Immunity in Arabidopsis.” *The Plant Cell* 23 (8): 2831–49. doi:10.1105/tpc.111.087122.
Lee, B h, R Johnston, Y Yang, A Gallavotti, M Kojima, B A N Travencolo, L d F Costa, H Sakakibara, and D Jackson. 2009. “Studies of Aberrant phyllotaxy1 Mutants of Maize Indicate Complex Interactions between Auxin and Cytokinin Signaling in the Shoot Apical Meristem.” *Plant Physiology* 150 (1): 205–16.
Lee, Byeong-ha, Robyn Johnston, Yan Yang, Andrea Gallavotti, Mikiko Kojima, Bruno A N Travençolo, Luciano da F Costa, Hitoshi Sakakibara, and David Jackson. 2009. “Studies of Aberrant phyllotaxy1 Mutants of Maize Indicate

Complex Interactions between Auxin and Cytokinin Signaling in the Shoot Apical Meristem." *Plant Physiology* 150 (1): 205–16. doi:10.1104/pp.109.137034.
Lee, Kwang Hee, Hai Lan Piao, Ho-Youn Kim, Sang Mi Choi, Fan Jiang, Wolfram Hartung, Ildoo Hwang, June M Kwak, In-Jung Lee, and Inhwan Hwang. 2006. "Activation of Glucosidase via Stress-Induced Polymerization Rapidly Increases Active Pools of Abscisic Acid." *Cell* 126 (6): 1109–20. doi:10.1016/j.cell.2006.07.034.
Lewis, Daniel R, Melissa V Ramirez, Nathan D Miller, Prashanthi Vallabhaneni, W Keith Ray, Richard F Helm, Brenda S J Winkel, and Gloria K Muday. 2011. "Auxin and Ethylene Induce Flavonol Accumulation through Distinct Transcriptional Networks." *Plant Physiology* 156 (1): 144–64. doi:10.1104/pp.111.172502.
Ludwig, Yvonne, Yanxiang Zhang, and Frank Hochholdinger. 2013. "The Maize (Zea Mays L.) AUXIN/INDOLE-3-ACETIC ACID Gene Family: Phylogeny, Synteny, and Unique Root-Type and Tissue-Specific Expression Patterns during Development." *PLoS ONE* 8 (11): 1–12. doi:10.1371/journal.pone.0078859.
McCarty, Donald R, Masaharu Suzuki, Charles Hunter, Joseph Collins, Wayne T Avigne, and Karen E Koch. 2013. "Genetic and Molecular Analyses of UniformMu Transposon Insertion Lines." *Methods in Molecular Biology (Clifton, N.J.)* 1057 (January): 157–66. doi:10.1007/978-1-62703-568-2_11.
McSteen, Paula, and Ottoline Leyser. 2005. "Shoot Branching." *Annual Review of Plant Biology* 56 (January): 353–74. doi:10.1146/annurev.arplant.56.032604.144122.
McSteen, Paula, Simon Malcomber, Andrea Skirpan, China Lunde, Xianting Wu, Elizabeth Kellogg, and Sarah Hake. 2007. "Barren inflorescence2 Encodes a Co-Ortholog of the PINOID Serine/threonine Kinase and Is Required for Organogenesis during Inflorescence and Vegetative Development in Maize." *Plant Physiology* 144 (2). Department of Biology, Pennsylvania State University, University Park, Pennsylvania 16802, USA. pcm11@psu.edu: 1000–1011. doi:10.1104/pp.107.098558.
Melan, M A, X Dong, M E Endara, K R Davis, F M Ausubel, and T K Peterman. 1993. "An Arabidopsis Thaliana Lipoxygenase Gene Can Be Induced by Pathogens, Abscisic Acid, and Methyl Jasmonate." *Plant Physiology* 101 (2): 441–50.
Mizukami, Y., and R. L. Fischer. 2000. "Plant Organ Size Control: AINTEGUMENTA Regulates Growth and Cell Numbers during Organogenesis." *Proceedings of the National Academy of Sciences* 97 (2): 942–47. doi:10.1073/pnas.97.2.942.
Morgante, M, and A M Olivieri. 1993. "PCR-Amplified Microsatellites as Markers in Plant Genetics." *The Plant Journal : For Cell and Molecular Biology* 3 (1): 175–82.
Murphy, Angus S, Karen R Hoogner, Wendy Ann Peer, and Lincoln Taiz. 2002. "Identification, Purification, and Molecular Cloning of N-1-Naphthylphthalmic Acid-Binding Plasma Membrane-Associated Aminopeptidases from

Arabidopsis." *Plant Physiology* 128 (3): 935–50. doi:10.1104/pp.010519.
Nanao, Max H, Thomas Vinos-Poyo, Géraldine Brunoud, Emmanuel Thévenon, Meryl Mazzoleni, David Mast, Stéphanie Lainé, et al. 2014. "Structural Basis for Oligomerization of Auxin Transcriptional Regulators." *Nature Communications* 5 (January): 3617. doi:10.1038/ncomms4617.
Neuffer, M G, Guri Johal, M T Chang, and Sarah Hake. 2009. "Handbook of Maize: Genetics and Genomics." In , edited by Jeffrey L Bennetzen and Sarah Hake, 63–84. New York, NY: Springer New York. doi:10.1007/978-0-387-77863-1_4.
Noh, B, A S Murphy, and E P Spalding. 2001. "Multidrug Resistance-like Genes of Arabidopsis Required for Auxin Transport and Auxin-Mediated Development." *The Plant Cell* 13 (11): 2441–54.
O'Connor, Devin L., Adam Runions, Aaron Sluis, Jennifer Bragg, John P. Vogel, Przemyslaw Prusinkiewicz, and Sarah Hake. 2014. "A Division in PIN-Mediated Auxin Patterning during Organ Initiation in Grasses." *PLoS Computational Biology* 10 (1): 21–24. doi:10.1371/journal.pcbi.1003447.
Okada, K, J Ueda, M K Komaki, and C J Bell. 1991. "Requirement of the Auxin Polar Transport System in Early Stages of Arabidopsis Floral Bud Formation." *The Plant Cell*. American Society of Plant Biologists.
Ouellet, F, P J Overvoorde, and A Theologis. 2001. "IAA17/AXR3: Biochemical Insight into an Auxin Mutant Phenotype." *The Plant Cell* 13 (4): 829–41.
Overvoorde, Paul J, Yoko Okushima, José M Alonso, April Chan, Charlie Chang, Joseph R Ecker, Beth Hughes, et al. 2005. "Functional Genomic Analysis of the AUXIN/INDOLE-3-ACETIC ACID Gene Family Members in Arabidopsis Thaliana." *The Plant Cell* 17 (12): 3282–3300. doi:10.1105/tpc.105.036723.
Padmanabhan, Meenu S, Haiymanot Shiferaw, and James N Culver. 2006. "The Tobacco Mosaic Virus Replicase Protein Disrupts the Localization and Function of Interacting Aux/IAA Proteins." *Molecular Plant-Microbe Interactions : MPMI* 19 (8): 864–73. doi:10.1094/MPMI-19-0864.
Peer, Wendy Ann. 2013. "From Perception to Attenuation: Auxin Signalling and Responses." *Current Opinion in Plant Biology* 16 (5): 561–68. doi:10.1016/j.pbi.2013.08.003.
Peer, Wendy Ann, Anindita Bandyopadhyay, Joshua J Blakeslee, Srinivas N Makam, Rujin J Chen, Patrick H Masson, and Angus S Murphy. 2004. "Variation in Expression and Protein Localization of the PIN Family of Auxin Efflux Facilitator Proteins in Flavonoid Mutants with Altered Auxin Transport in Arabidopsis Thaliana." *The Plant Cell* 16 (7): 1898–1911. doi:10.1105/tpc.021501.
Peer, Wendy Ann, Joshua J. Blakeslee, Haibing Yang, and Angus S. Murphy. 2011. "Seven Things We Think We Know about Auxin Transport." *Molecular Plant* 4 (3). The Authors 2011.: 487–504. doi:10.1093/mp/ssr034.
Petrášek, Jan, Jozef Mravec, Rodolphe Bouchard, Joshua J Blakeslee, Melinda Abas, Daniela Seifertova, Justyna Wiśniewska, et al. 2006. "PIN Proteins Perform a Rate-Limiting Function in Cellular Auxin Efflux." *Science Signaling* 312 (5775). AAAS: 914.
Poethig, R S. 1988. "Heterochronic Mutations Affecting Shoot Development in

Maize.” *Genetics* 119 (4): 959–73.
Ramos, J A, N Zenser, O Leyser, and J Callis. 2001. “Rapid Degradation of Auxin/indoleacetic Acid Proteins Requires Conserved Amino Acids of Domain II and Is Proteasome Dependent.” *The Plant Cell* 13 (10): 2349–60.
Reed, Jason W. 2001. “Roles and Activities of Aux/IAA Proteins in Arabidopsis.” *Trends in Plant Science* 6 (9): 420–25. doi:10.1016/S1360-1385(01)02042-8.
Rodríguez, Andrés Alberto, Santiago Javier Maiale, Ana Bernardina Menéndez, and Oscar Adolfo Ruiz. 2009. “Polyamine Oxidase Activity Contributes to Sustain Maize Leaf Elongation under Saline Stress.” *Journal of Experimental Botany* 60 (15): 4249–62. doi:10.1093/jxb/erp256.
Roepke, Jonathon, and Gale G. Bozzo. 2015. “Arabidopsis Thaliana β-Glucosidase BGLU15 Attacks Flavonol 3-O-β-Glucoside-7-O-α-Rhamnosides.” *Phytochemistry* 109. Elsevier Ltd: 14–24. doi:10.1016/j.phytochem.2014.10.028.
Rubery, P H, and A R Sheldrake. 1974. “Carrier-Mediated Auxin Transport.” *Planta* 118 (2): 101–21. doi:10.1007/BF00388387.
Růzicka, Kamil, Karin Ljung, Steffen Vanneste, Radka Podhorská, Tom Beeckman, Jirí Friml, and Eva Benková. 2007. “Ethylene Regulates Root Growth through Effects on Auxin Biosynthesis and Transport-Dependent Auxin Distribution.” *The Plant Cell* 19 (7): 2197–2212. doi:10.1105/tpc.107.052126.
Saito, Kazuki, Keiko Yonekura-Sakakibara, Ryo Nakabayashi, Yasuhiro Higashi, Mami Yamazaki, Takayuki Tohge, and Alisdair R Fernie. 2013. “The Flavonoid Biosynthetic Pathway in Arabidopsis: Structural and Genetic Diversity.” *Plant Physiology and Biochemistry : PPB / Société Francaise de Physiologie Végétale* 72 (November): 21–34. doi:10.1016/j.plaphy.2013.02.001.
Santelia, Diana, Sina Henrichs, Vincent Vincenzetti, Michael Sauer, Laurent Bigler, Markus Klein, Aurélien Bailly, et al. 2008. “Flavonoids Redirect PIN-Mediated Polar Auxin Fluxes during Root Gravitropic Responses.” *The Journal of Biological Chemistry* 283 (45): 31218–26. doi:10.1074/jbc.M710122200.
Saslowsky, David E, Ujwala Warek, and Brenda S J Winkel. 2005. “Nuclear Localization of Flavonoid Enzymes in Arabidopsis.” *The Journal of Biological Chemistry* 280 (25): 23735–40. doi:10.1074/jbc.M413506200.
Sharopova, Natalya, Michael D McMullen, Linda Schultz, Steve Schroeder, Hector Sanchez-Villeda, Jack Gardiner, Dean Bergstrom, et al. “Development and Mapping of SSR Markers for Maize.” *Plant Molecular Biology* 48 (5-6): 463–81.
Snow, Mary, and R Snow. 1932. “Experiments on Phyllotaxis. I. The Effect of Isolating a Primordium.” *Philosophical Transactions of the Royal Society of London. Series B, Containing Papers of a Biological Character* 221. The Royal Society: 1–43.
Stahle, Melissa I, Janine Kuehlich, Lindsay Staron, Albrecht G von Arnim, and John F Golz. 2009. “YABBYs and the Transcriptional Corepressors LEUNIG

and LEUNIG_HOMOLOG Maintain Leaf Polarity and Meristem Activity in Arabidopsis." *The Plant Cell* 21 (10): 3105–18. doi:10.1105/tpc.109.070458.
Su, Ying-Hua, Yu-Bo Liu, and Xian-Sheng Zhang. 2011. "Auxin-Cytokinin Interaction Regulates Meristem Development." *Molecular Plant* 4 (4): 616–25. doi:10.1093/mp/ssr007.
Szemenyei, Heidi, Mike Hannon, and Jeff A Long. 2008. "TOPLESS Mediates Auxin-Dependent Transcriptional Repression during Arabidopsis Embryogenesis." *Science (New York, N.Y.)* 319 (5868): 1384–86. doi:10.1126/science.1151461.
Tassoni, Annalisa, Marianne van Buuren, Marina Franceschetti, Silvia Fornalè, and Nello Bagni. 2000. "Polyamine Content and Metabolism in Arabidopsis Thaliana and Effect of Spermidine on Plant Development." *Plant Physiology and Biochemistry* 38 (5): 383–93. doi:10.1016/S0981-9428(00)00757-9.
Thompson, Addie M, Jianming Yu, Marja C P Timmermans, Patrick Schnable, James C Crants, Michael J Scanlon, and Gary J Muehlbauer. 2015. "Diversity of Maize Shoot Apical Meristem Architecture and Its Relationship to Plant Morphology." *G3 (Bethesda, Md.)* 5 (5): 819–27. doi:10.1534/g3.115.017541.
Tian, Qing, Nicholas J Uhlir, and Jason W Reed. 2002. "Arabidopsis SHY2/IAA3 Inhibits Auxin-Regulated Gene Expression." *The Plant Cell* 14 (2): 301–19.
Tiwari, Shiv B, Gretchen Hagen, and Tom J Guilfoyle. 2004. "Aux/IAA Proteins Contain a Potent Transcriptional Repression Domain." *The Plant Cell* 16 (2): 533–43. doi:10.1105/tpc.017384.
Trapnell, Cole, Brian A Williams, Geo Pertea, Ali Mortazavi, Gordon Kwan, Marijke J van Baren, Steven L Salzberg, Barbara J Wold, and Lior Pachter. 2010. "Transcript Assembly and Quantification by RNA-Seq Reveals Unannotated Transcripts and Isoform Switching during Cell Differentiation." *Nature Biotechnology* 28 (5). NIH Public Access: 511–15. doi:10.1038/nbt.1621.
Tsuda, Katsutoshi, Yukihiro Ito, Yutaka Sato, and Nori Kurata. 2011. "Positive Autoregulation of a KNOX Gene Is Essential for Shoot Apical Meristem Maintenance in Rice." *The Plant Cell* 23 (12): 4368–81. doi:10.1105/tpc.111.090050.
Ulmasov, T, G Hagen, and T J Guilfoyle. 1997. "ARF1, a Transcription Factor That Binds to Auxin Response Elements." *Science (New York, N.Y.)* 276 (5320): 1865–68.
Ulmasov, T, Z B Liu, G Hagen, and T J Guilfoyle. 1995. "Composite Structure of Auxin Response Elements." *The Plant Cell* 7 (10): 1611–23. doi:10.1105/tpc.7.10.1611.
Vernoux, T, J Kronenberger, O Grandjean, P Laufs, and J Traas. 2000. "PIN-FORMED 1 Regulates Cell Fate at the Periphery of the Shoot Apical Meristem." *Development* 127 (23). The Company of Biologists Limited: 5157–65.
Vieten, Anne, Steffen Vanneste, Justyna Wisniewska, Eva Benková, René Benjamins, Tom Beeckman, Christian Luschnig, and Jirí Friml. 2005. "Functional Redundancy of PIN Proteins Is Accompanied by Auxin-

Dependent Cross-Regulation of PIN Expression." *Development (Cambridge, England)* 132 (20): 4521–31. doi:10.1242/dev.02027.
Vollbrecht, E, L Reiser, and S Hake. 2000. "Shoot Meristem Size Is Dependent on Inbred Background and Presence of the Maize Homeobox Gene, knotted1." *Development (Cambridge, England)* 127 (14): 3161–72.
Wabnik, Krzysztof, Jürgen Kleine-Vehn, Willy Govaerts, and Jiří Friml. 2011. "Prototype Cell-to-Cell Auxin Transport Mechanism by Intracellular Auxin Compartmentalization." *Trends in Plant Science* 16 (9): 468–75. doi:10.1016/j.tplants.2011.05.002.
Wang, Lin, Yaqing Si, Lauren K Dedow, Ying Shao, Peng Liu, and Thomas P Brutnell. 2011. "A Low-Cost Library Construction Protocol and Data Analysis Pipeline for Illumina-Based Strand-Specific Multiplex RNA-Seq." *PloS One* 6 (10). Public Library of Science: e26426. doi:10.1371/journal.pone.0026426.
Wang, Renhou, and Mark Estelle. 2014. "Diversity and Specificity: Auxin Perception and Signaling through the TIR1/AFB Pathway." *Current Opinion in Plant Biology* 21 (October): 51–58. doi:10.1016/j.pbi.2014.06.006.
Wang, Zhong, Mark Gerstein, and Michael Snyder. 2009. "RNA-Seq: A Revolutionary Tool for Transcriptomics." *Nature Reviews. Genetics* 10 (1): 57–63. doi:10.1038/nrg2484.
Worley, C K, N Zenser, J Ramos, D Rouse, O Leyser, A Theologis, and J Callis. 2000. "Degradation of Aux/IAA Proteins Is Essential for Normal Auxin Signalling." *The Plant Journal : For Cell and Molecular Biology* 21 (6): 553–62.
Wu, Thomas D, and Serban Nacu. 2010. "Fast and SNP-Tolerant Detection of Complex Variants and Splicing in Short Reads." *Bioinformatics (Oxford, England)* 26 (7): 873–81. doi:10.1093/bioinformatics/btq057.
Wu, Thomas D, and Colin K Watanabe. 2005. "GMAP: A Genomic Mapping and Alignment Program for mRNA and EST Sequences." *Bioinformatics (Oxford, England)* 21 (9): 1859–75. doi:10.1093/bioinformatics/bti310.
Xie, Q, G Frugis, D Colgan, and N H Chua. 2000. "Arabidopsis NAC1 Transduces Auxin Signal Downstream of TIR1 to Promote Lateral Root Development." *Genes & Development* 14 (23): 3024–36.
Xie, Qi, Hui-Shan Guo, Geza Dallman, Shengyun Fang, Allan M Weissman, and Nam-Hai Chua. 2002. "SINAT5 Promotes Ubiquitin-Related Degradation of NAC1 to Attenuate Auxin Signals." *Nature* 419 (6903). Macmillian Magazines Ltd.: 167–70. doi:10.1038/nature00998.
Xu, Jing, Zhen-Hong Su, Chen Chen, Hong-Juan Han, Bo Zhu, Xiao-Yan Fu, Wei Zhao, Xiao-Fen Jin, Ai-Zhong Wu, and Quan-Hong Yao. 2012. "Stress Responses to Phenol in Arabidopsis and Transcriptional Changes Revealed by Microarray Analysis." *Planta* 235 (2): 399–410. doi:10.1007/s00425-011-1498-5.
Xue, Beibei, Aying Zhang, and Mingyi Jiang. 2009. "Involvement of Polyamine Oxidase in Abscisic Acid-Induced Cytosolic Antioxidant Defense in Leaves of Maize." *Journal of Integrative Plant Biology* 51 (3): 225–34. doi:10.1111/j.1744-7909.2008.00766.x.
Yeh, Su-Ying, Hau-Wen Chen, Chun-Yeung Ng, Chu-Yin Lin, Tung-Hai Tseng,

Wen-Hsiung Li, and Maurice S B Ku. 2015. “Down-Regulation of Cytokinin Oxidase 2 Expression Increases Tiller Number and Improves Rice Yield.” *Rice (New York, N.Y.)* 8 (1): 36. doi:10.1186/s12284-015-0070-5.

Yin, Ruohe, Kerstin Han, Werner Heller, Andreas Albert, Petre I. Dobrev, Eva Zažímalová, and Anton R. Schäffner. 2014. “Kaempferol 3-O-Rhamnoside-7-O-Rhamnoside Is an Endogenous Flavonol Inhibitor of Polar Auxin Transport in Arabidopsis Shoots.” *New Phytologist* 201 (2): 466–75. doi:10.1111/nph.12558.

Zažímalová, E, A S Murphy, H Yang, K Hoyerová, and P Hošek. 2010. “Auxin Transporters—Why So Many?” *Cold Spring Harbor Perspectives in Biology* 2 (3). Cold Spring Harbor Lab.